J Geophys (1985) 57:191-206

Journal of Geophysics

# Construction of conductance bounds from magnetotelluric impedances

**P. Weidelt**

Institut für Geophysik und Meteorologie, Technische Universität, Mendelssohnstraße 3, D-3300 Braunschweig, Federal Republic of Germany

**Abstract.** Whereas any finite set of impedance data does not constrain the electrical conductivity $\sigma(z)$ at a fixed level $z$ in a $1D$-model, the conductance function $S(z_2)$ as the depth-integrated conductivity from the surface to the depth $z_2$ will be constrained. Assuming only the non-negativity of $\sigma(z)$, it is shown that for a given depth $z_2$ the models generating the lower and upper bound of $S(z_2)$ consist of a sequence of thin sheets. The determination of the positions of the thin sheets and their conductances leads to a system of nonlinear equations. As a limitation the present approach requires the existence of a model, which exactly fits the data. The structure of the extermal models as a function of $z_2$ is discussed in examples with a small number of frequencies. Moreover, it is shown that any set of complex $1D$ impedances for $M$ frequencies can be represented by a partial fraction expansion involving not more than $2M$ (positive) constants. For exactly $2M$ constants there are two complementary representations related to the lower and upper bound of $S(z_2)$.

For the simple one-frequency case, a more general extremal problem is briefly considered, where the admitted conductivities are constrained by a priori bounds $\sigma_-(z)$ and $\sigma_+(z)$ such that $\sigma_-(z) \leqq \sigma(z) \leqq \sigma_+(z)$. In this case, the extremal models for $S(z_2)$ consist of a sequence of sections with alternating conductivities $\sigma_-(z)$ and $\sigma_+(z)$. The sharpening of conductance bounds by incorporating a priori information is illustrated by an example.

**Key words:** Electromagnetic induction – Inverse problem – Extremal models

## 1. Introduction

The $1D$-magnetotelluric inverse problem is known to be ill-posed and thus allows the construction of a whole set of satisfactory conductivity models from a given real data set. The COPROD study of Jones (1980) provides a good illustration of this fact. At present there are two attempts to overcome the problem: either the inversion is stabilized by incorporating known or assumed properties of the conductivity structure as a priori constraints, or one may try to extract geophysically useful properties pertaining to the whole class of conductivity models consistent with the data. In principle, the latter problem can be approached either by exploring the whole space of feasible models by Monte Carlo techniques or by explicitly constructing the model, which extremizes the geophysically interesting property. Firm foundations for the use of the Monte Carlo method as a tool for geophysical inverstion were laid by Anderssen and Seneta (1971, 1972) and the method of parameter extremization in geophysical inverse problems was pioneered by Parker (1972, 1974, 1975).

Any set of magnetotelluric impedances for a finite number of frequencies does not impose bounds on the conductivity $\sigma(z)$ at any fixed depth $z$. At this depth, either a thin insulating sheet or a sheet of unbounded conductivity, but of finite conductance (conductivity thickness product), may exist. However, conductivity *averages* over a finite depth range will, in general, be constrained by the data, provided the field penetrates down to this depth. This has been exemplified in detail by Oldenburg (1983), who constructed bounds on conductivity averages by linearizing the nonlinear problem. The existence of bounds for conductivity averages or for the simpler conductance function

$$S(z_2) = \int_0^{z_2} \sigma(z)\,dz \qquad (1.1)$$

reflects the fact that the inverse problem for $S(z_2)$ is well-posed (V.I. Dmitriev, private communication).

The present study is centered on the computation of bounds for $S(z_2)$, imposing apart from the non-negativity condition $\sigma(z) \geqq 0$ no further constraints on the conductivity. Any model consistent with the data must lie within these bounds. The problem under consideration resembles the problem of discovering extremal models of linear functionals of the density from a truncated set of eigenfrequencies of an elastic string, as treated by Barcilon (1979), Barcilon and Turchetti (1979), and Sabatier (1979). Briefly addressed is also the more general problem of computing bounds for conductivity averages rather than for $S(z_2)$.

We shall consider only for the simple one-frequency case the construction of bounds for $S(z_2)$ when $\sigma(z)$ is constrained by a priori bounds $\sigma_-(z)$ and $\sigma_+(z)$ such that $\sigma_-(z) \leqq \sigma(z) \leqq \sigma_+(z)$.

Contrary to the pragmatic approach of Oldenburg (1983), who applies his approximate method to a large number of frequencies, attention is confined in this very preliminary study to the exact extremal models for a small number of impedances. We also have to assume that there is a model that fits the data exactly. This restriction, however, may be dropped in subsequent work, thus extending the range of applicability to real inconsistent data sets. Only in connection with the COPROD study are approximate extremal models for many real data considered.

Although the present problem is one of the simplest extremal problems in electromagnetic induction, the nonlinearity introduces a great deal of complexity and leaves the treatment still in an experimental stage. Another relatively simple extremal problem in electromagnetic induction can be solved for two-dimensional perfect conductors (Weidelt, 1981).

The main part of the paper consists of three sections. The general structure of the extremal models is derived in Sect. 2. Then a detailed discussion and illustration of unconstrained extremal models is given in Sect. 3, and the concluding Sect. 4 is devoted to simple extremal models with a priori constraints on conductivity. The paper has two appendices, where in particular Appendix B contains the proof of an impedance representation theorem, to which we have to appeal in Sect. 3.

## 2. Necessary conditions for extremal models

Assuming *SI* units, a time factor $e^{i\omega t}$, a $1D$-conductivity structure $\sigma(z)$, and neglecting displacement currents, Maxwell's equations reduce for a quasi-uniform incident magnetic field in the $y$-direction to

$$E_x'(z,\omega) = -i\omega\mu_0 H_y(z,\omega), \quad H_y'(z,\omega) = -\sigma(z) E_x(z,\omega), \tag{2.1}$$

implying

$$f''(z,\omega) = i\omega\mu_0\sigma(z) f(z,\omega), \tag{2.2}$$

where $f(z) := E_x(z,\omega)$. In the sequel we use the transfer function $c$ introduced by Schmucker (1970). Its theoretical value for given $\sigma(z)$ at a set of $M$ frequencies $\omega_j$, $j=1,\ldots,M$ is defined as

$$c_j[\sigma] = \frac{E_x(0.\,\omega_j)}{i\omega_j\mu_0 H_y(-0,\omega_j)} = -\frac{f(0,\omega_j)}{f'(-0,\omega_j)}, \tag{2.3}$$

where $f(z)$ is a solution of Eq. (2.2), with $f'(z)\to 0$ for $z\to\infty$. In Eq. (2.3), provision is made for a possible discontinuity of $H_y$ or $f'$ at $z=0$ due to the presence of a thin conducting sheet. The $M$ complex data $c_j$, which are assumed for the present to be exact, correspond to the functionals $c_j[\sigma]$. Then the problem of interpretation consists in finding at least one model $\sigma(z)$ such that $c_j[\sigma]=c_j$, $j=1,\ldots,M$. When there is no risk of confusing functionals and data, $[\sigma]$ is omitted.

Within the class of models fitting the finite data set we are interested in those two models, which minimize and maximize either for a given depth range $z_1 \leqq z \leqq z_2$ the conductivity average

$$\bar{\sigma}(z_1,z_2) = \frac{1}{z_2-z_1}\int_{z_1}^{z_2} \sigma(z)\,dz \tag{2.4a}$$

or simpler for a given $z_2>0$ the conductance function

$$S(z_2) = \int_0^{z_2} \sigma(z)\,dz. \tag{2.4b}$$

These four cases are equivalent to the problem of *minimizing* the objective function

$$Q[\sigma] = \int_0^{\infty} w(z)\sigma(z)\,dz \tag{2.5}$$

with the weights

$$w(z) = \begin{cases} 0, & 0\leqq z<z_1 \quad \text{and } z>z_2 \\ \dfrac{1}{z_2-z_1}, & z_1\leqq z\leqq z_2 \quad \text{for } Q=\bar{\sigma}_{\min} \\ \dfrac{-1}{z_2-z_1}, & z_1\leqq z\leqq z_2 \quad \text{for } Q=-\bar{\sigma}_{\max} \end{cases} \tag{2.6a}$$

or

$$w(z) = \begin{cases} 1, & 0\leqq z\leqq z_2 \quad \text{for } Q=S_{\min} \\ -1, & 0\leqq z\leqq z_2 \quad \text{for } Q=-S_{\max} \\ 0, & z>z_2 \end{cases} \tag{2.6b}$$

Assuming that $\sigma(z)$ is only constrained by the non-negativity condition, we are faced with the nonlinear programming problem of minimizing $Q[\sigma]$ subject to the constraints

$$c_j[\sigma] = c_j, \quad j=1,\ldots,M \tag{2.7a}$$

and

$$\sigma(z) \geqq 0. \tag{2.7b}$$

The equality constraints (2.7a) render the problem nonlinear. The Lagrange function is

$$L[\sigma] = Q[\sigma] + \operatorname{Re}\sum_{j=1}^{M} \lambda_i\{c_j[\sigma]-c_j\} - \int_0^{\infty} \mu(z)\sigma(z)\,dz, \tag{2.8}$$

where the $M$ complex Lagrangian multipliers $\lambda_j$ enforce the equality constraints, whereas the non-negative function $\mu(z)$ takes the inequality constraint into account and satisfies

$$\mu(z)=0,\ \sigma(z)>0; \quad \mu(z)\geqq 0,\ \sigma(z)=0 \tag{2.9}$$

(e.g., Pearson, 1974, p. 1113). The formally introduced Lagrangian multipliers $\lambda_j$ can be interpreted as the sensitivity of the minimum value $Q_0$ of the objective functional $Q[\sigma]$ to changes in the constraining data $c_j = g_j - ih_j$ (e.g., Pearson, 1974, p. 1118):

$$\operatorname{Re}\lambda_i = -\frac{\partial Q_0}{\partial g_j}, \quad \operatorname{Im}\lambda_j = -\frac{\partial Q_0}{\partial h_j}. \tag{2.10}$$

Hence, the $\lambda_j$ allow immediately a rough estimate of the influence of data errors. Also $\mu(z)$ can be interpreted as the sensitivity of $Q_0$ by changing the lower bound of $\sigma(z)$ in the neighborhood of $z$ to a positive value: let $\sigma(\zeta)\geqq\tilde{\sigma}_-(\zeta)$ in $z-\Delta z/2\leqq\zeta\leqq z+\Delta z/2$ and let

$$\Delta\tau = \int_{z-\Delta z/2}^{z+\Delta z/2} \tilde{\sigma}_-(\zeta)\,d\zeta.$$

Then we obtain in the limit $\Delta z \to 0$

$$\mu(z) = \frac{\partial Q_0}{\partial \tau}, \tag{2.11}$$

i.e. $Q_0$ is not affected, if the constraint is not binding ($\sigma(z) > 0$, $\mu(z) = 0$) and $Q_0$ will not decrease for a binding constraint ($\sigma(z) = 0$, $\mu(z) \geqq 0$). These results, of course, were expected.

As a *necessary* condition for an extremum of $Q$, the first variation of $L$ with respect to $\sigma$ has to vanish. This yields

$$w(z) + \mathrm{Re} \sum_{j=1}^{M} \lambda_j F_j(z) - \mu(z) = 0, \tag{2.12}$$

where $F_j(z)$ is the Fréchet derivative of the functional $c_j[\sigma]$, defined by

$$\delta c_j[\sigma] = \int_0^\infty F_j(z) \delta\sigma(z) dz \tag{2.13}$$

with

$$F_j(z) = -i\omega\mu_0 f_j^2(z) \tag{2.14}$$

(e.g., Parker, 1977), where $f_j(z) := f(z, \omega_j)$ is the solution of Eq. (2.2) with $f_j'(-0) = 1$ and $f_j'(z) \to 0$ for $z \to \infty$. The lowest-order differential equations satisfied by $F_j(z)$ are

$$2F_j F_j'' = 4i\omega_j \mu_0 \sigma F_j^2 + (F_j')^2, \tag{2.15a}$$

$$F_j''' = 4i\omega_j \mu_0 \sqrt{\sigma} (\sqrt{\sigma} F_j)'. \tag{2.15b}$$

On using Eq. (2.12), a function $D(z)$ is defined as

$$D(z) := w(z) + \mathrm{Re} \sum_{j=1}^{M} \lambda_j F_j(z) = \mu(z). \tag{2.16}$$

Now assume that in some interval $a < z < b$, completely inside an interval where $w(z)$ is constant, the conductivity $\sigma(z)$ is positive, i.e., $\sigma(z) > 0$ for $z \in (a, b)$. Then from Eq. (2.9) $\mu(z) = 0$ for $z \in (a, b)$ and Eq. (2.12) reads

$$D(z) = 0, \quad z \in (a, b). \tag{2.17}$$

In Appendix A it is shown that for downward diffusing fields $F_j(z)$ this equation has no solution, except for the trivial solution $\lambda_j = 0$ if $w(z) = 0$ for $z > a$. For $M = 1$ this can be verified easily: since Eq. (2.17) holds in a whole interval, it can be differentiated an arbitrary number of times. In particular, the first two derivatives at $z \in (a, b)$ read (skipping the subscript 1)

$$D' = -2\mathrm{Re}\{2F/c\} = 0,$$

$$D'' = +\mathrm{Re}\{\lambda F(i\omega\mu_0\sigma + 1/c^2)\} = 0$$

with $c = c(z) = -f(z)/f'(z) = g - ih$, $g > 0$, $h > 0$ for a downward diffusing field. The above equations can be considered as two linear homogeneous equations for $\mathrm{Re}(\lambda F)$ and $\mathrm{Im}(\lambda F)$, admitting a nontrivial solution only for a vanishing system determinant $\Delta$. However,

$$|\Delta| = 4(h + \omega\mu_0\sigma g |c|^2)/|c|^4 > 0.$$

The linear independence of the Fréchet derivatives has the important consequence that the extremal models cannot comprise conductivity sections, where $\sigma(z)$ is positive over a *finite* interval. Therefore, the extremal models consist of a sequence of insulating layers ($\sigma = 0$) and thin conducting sheets, where $\sigma(z)$ is positive only at an isolated point.

The problem of model construction consists in finding for a given impedance set a sequence of thin sheets and a set of complex Lagrangian multipliers such that the model fits the data and the function $D(z)$ is nonnegative everywhere and in particular vanishes at the positions of the thin sheets, i.e.,

$$D(z) \geqq 0; \quad D(z) = 0 \quad \text{for } \sigma(z) > 0. \tag{2.18}$$

This is clearly a nonlinear problem, since both the data functionals and the Fréchet derivatives depend nonlinearly on the positions and conductances of the thin sheets. Also, it is not yet clear from the outset how many sheets have to be considered. (Semi-empirical rules derived from experience with a small number of frequencies are listed in Sect. 3.6.) Concerning the nonnegativity of $D(z)$, closer examination in Sect. 3.3 shows that for $z < z_2$ we have $D(z) > 0$, for $\sigma(z) = 0$, and $D(z) = 0$ for $\sigma(z) > 0$, whereas $D(z)$ vanishes identically below the first sheet occurring in $z > z_2$.

In a more general approach, the incorporation of a priori bounds $\sigma_-(z)$ and $\sigma_+(z)$ such that $\sigma_-(z) \leqq \sigma(z) \leqq \sigma_+(z)$ can be achieved by replacing the last term in the Lagrange function Eq. (2.8) by

$$-\int_0^\infty [\mu_+(z)\{\sigma_+(z) - \sigma(z)\} + \mu_-(z)\{\sigma(z) - \sigma_-(z)\}] dz,$$

where $\mu_\pm(z) \geqq 0$. Then the definition of $D(z)$ in analogy to Eq. (2.16) is

$$D(z) = \mu_-(z) - \mu_+(z). \tag{2.19}$$

$D(z)$ vanishes, if $\sigma(z)$ attains neither its lower nor its upper bound. For the one-frequency case it was shown above that $D(z)$ cannot vanish in a finite interval. Therefore, in this case the extremal models consist of a stack of sections with alternating conductivities $\sigma_-(z)$ and $\sigma_+(z)$, satisfying

$$\left.\begin{matrix} \sigma(z) = \sigma_+(z) \\ \sigma(z) = \sigma_-(z) \end{matrix}\right\} \quad \text{for } D(z) \begin{cases} \leqq 0 \\ \geqq 0 \end{cases}. \tag{2.20}$$

Jumps between $\sigma_-$ and $\sigma_+$ occur, where $D(z)$ changes sign. The generalization to $M$ frequencies must still be done, but it can be anticipated from the approximate extremal models presented by Oldenburg (1983) in his Fig. 7 that also in this case only the conductivities $\sigma_-$ and $\sigma_+$ will occur.

## 3. Extremal models for the unconstrained conductance function

### 3.1 *Formulas for a series of thin sheets*

The discussion is started with the unconstrained extremal models requiring only the assumption $\sigma(z) \geqq 0$, and attention is confined to the conductance function in Eq. (1.1)

$$S(z_2) = \int_0^{z_2} \sigma(z) dz \tag{3.1}$$

rather than considering conductivity averages. In the unconstrained case the extremal models reduce to a series of thin sheets. Models of this kind have been identified previously by Parker (1980) as giving the best fit to any real data set.

Formulas for the treatment of a series of thin sheets are briefly summarized. Assume a stack of $K$ sheets with conductance $\tau_k$ at depth $\zeta_k$, i.e.,

$$\sigma(z)=\sum_{k=1}^{K}\tau_k\delta(z-\zeta_k).$$

The inter-sheet separations are $d_k=\zeta_k-\zeta_{k-1}$, $k=2,\dots,K$. Then the solution $f(z)$ of (2.2) varies linearly between two sheets, is continuous at $z=\zeta_k$, but shows the discontinuous slope

$$f'(\zeta_k+0)-f'(\zeta_k-0)=i\omega\mu_0\tau_k f(\zeta_k),\quad k=1,\dots,K \tag{3.2}$$

$f(z)$ is constant in $z\geq\zeta_K$, i.e. $f'(\zeta_K+0)=0$. The theoretical transfer function $c[\sigma]=-f(0)/f'(-0)$ is obtained as $c[\sigma]=c_1+\zeta_1$ with $c_k:=-f(\zeta_k)/f'(\zeta_k-0)$ recursively from

$$c_k=\frac{c_{k+1}+d_{k+1}}{1+i\omega\mu_0\tau_k(c_{k+1}+d_{k+1})},\quad k=K-1,\dots,1, \tag{3.3}$$

starting with $c_K=1/(i\omega\mu_0\tau_K)$. (In this section the subscript $k$ on $c$ denotes the value of $c$ at $z=\zeta_k-0$, whereas in a different context the subscript $j$ specifies the particular frequency $\omega_j$ of $c$ at $z=-0$.) The value of $f$ at $z=\zeta_k$, normalized to $f'(-0)=1$ is

$$f(\zeta_1)=-c_1,$$
$$f(\zeta_k)=f(\zeta_1)\prod_{n=2}^{k}\frac{c_n}{c_n+d_n},\quad k>1, \tag{3.4}$$

and the values of $f'(\zeta_k-0)=f'(\zeta_{k-1}+0)$ are determined from

$$f'(\zeta_1-0)=1,$$
$$f'(\zeta_k-0)=\prod_{n=1}^{k-1}(1-i\omega\mu_0\tau_n c_n),\quad k>1. \tag{3.5}$$

The partial derivatives of $c$ with respect to the model parameters $\tau_k$ and $\zeta_k$ are obtained by means of Eqs. (2.13) and (2.14):

$$\frac{\partial c[\sigma]}{\partial\tau_k}=F(\zeta_k)=-i\omega\mu_0 f^2(\zeta_k), \tag{3.6a}$$

$$\frac{\partial c[\sigma]}{\partial\zeta_k}=\tau_k\bar{F}'(\zeta_k)=[f'(\zeta_k-0)]^2-[f'(\zeta_k+0)]^2,\quad k=1,\dots,K-1 \tag{3.6b}$$

$$\frac{\partial c[\sigma]}{\partial\zeta_K}=\tfrac{1}{2}\tau_K F'(\zeta_K-0)=[f'(\zeta_K-0)]^2, \tag{3.6c}$$

where

$$\bar{F}'(\zeta_k)=\tfrac{1}{2}[F'(\zeta_k-0)+F'(\zeta_k+0)]. \tag{3.7}$$

*3.2 An impedance representation theorem*

The theoretical transfer function of a $1D$ conductivity distribution admits the spectral expansion

$$c[\sigma]=a_0+\int_0^\infty\frac{a(\lambda)d\lambda}{\lambda+i\omega},\quad a_0\geq 0,\ a(\lambda)\geq 0, \tag{3.8}$$

where $a(\lambda)$ is a generalized function to include both the discrete and continuous part of the spectrum (Weidelt, 1972; Parker, 1980; Parker and Whaler, 1981). As an example, the stack of thin sheets considered in the previous section has a finite discrete spectrum and leads to the representation

$$c[\sigma]=\zeta_1+\sum_{k=1}^{K-1}\frac{a_k}{b_k+i\omega}+\frac{a_K}{i\omega};$$
$$a_k,b_k>0;\ \zeta_1,a_K\geq 0. \tag{3.9}$$

Let the theoretical impedances $c_j[\sigma]$ for $M$ distinct frequencies $\omega_j$ be given by

$$c_j[\sigma]=a_0+\sum_{n=1}^{N}\frac{a_n}{b_n+i\omega_j} \tag{3.10}$$

with $a_n,b_n>0$, $n=1,\dots,N-1$; $a_0$, $b_N\geq 0$, where the $b_n$, $n=1,\dots,N$ are distinct. [This form rather than Eq. (3.8) is chosen for ease of presentation only, for equivalent integral analogs based on (3.8) exist for all formulas involving the summation over $n$.] Then for $N\geq M$ $c_j[\sigma]$ allows the two representations

$$\text{I: }c_j[\sigma]=\sum_{m=1}^{M}\frac{A_m}{B_m+i\omega_j}, \tag{3.11a}$$

$$\text{II: }c_j[\sigma]=\bar{A}_0+\sum_{m=1}^{M-1}\frac{\bar{A}_m}{\bar{B}_m+i\omega_j}+\frac{\bar{A}_M}{i\omega_j}, \tag{3.11b}$$

where all constants $A_m$, $B_m$, $\bar{A}_0$, $\bar{A}_m$, $\bar{B}_m$, and $\bar{A}_M$ are positive. For $N<M$ there is no representation other than Eq. (3.10). [See also Parker (1980).] The proofs are given in Appendix B.

Model I is a series of $M+1$ thin sheets: the first sheet is at $z=0$ and the last sheet has an infinite conductance. Complementary model II consists of $M$ thin sheets: the first sheet lies at $z=\bar{A}_0>0$ and the last sheet has a bounded conductance. Between models I and II is a duality relationship in the sense that they can be transformed into each other by replacing a sheet of finite (infinite) conductance by an insulating layer of finite (infinite) thickness, and vice versa.

Assuming the ordering $b_n>b_{n+1}$, $\bar{B}_m>\bar{B}_{m+1}$, we infer from (B-19, 20), (B-24), and (B-26) the inequalities

$$\sum_{m=1}^{M}(A_m/B_m)\leq a_0+\sum_{n=1}^{N}(a_n/b_n), \tag{3.12a}$$

$$\sum_{m=1}^{M}A_m\leq\sum_{n=1}^{N}a_n\quad(a_0=0), \tag{3.12b}$$

$$\bar{A}_0\geq a_0, \tag{3.12c}$$

$$\bar{A}_M\geq a_N\quad(b_N=0). \tag{3.12d}$$

These inequalities express the extremal properties of models I and II, with the following physical interpretation:

a) The depth of a perfect conductor (if present) is given by

$$z_\infty=\lim_{\omega\to 0}c(\omega). \tag{3.13a}$$

Hence Eq. (3.12a) implies that I is the model with the *shallowest* perfect conductor consistent with the data. Its position marks "the limiting depth below which nothing can be learnt about the conductivity" (Parker, 1982).

b) The conductance of a surface sheet, the presence of which requires $a_0=0$, is given by

$$S(+0)=\lim_{\omega\to\infty}\frac{1}{i\omega\mu_0 c(\omega)}. \tag{3.13b}$$

Hence Eq. (3.12b) says that model I has the *greatest* surface conductance.

c) The depth to the first conductor is

$$z_0=\lim_{\omega\to\infty} c(\omega). \tag{3.13c}$$

Therefore according to Eq. (3.12c), model II is the conductivity structure with the *deepest* top.

d) The total conductance in the absence of a perfect conductor ($b_N=0$) is

$$S(\infty)=\lim_{\omega\to 0}\frac{1}{i\omega\mu_0 c(\omega)}. \tag{3.13d}$$

Hence, Eq. (3.12d) implies that model II has the *least* total conductance of all models fitting the data.

The presentation of Eqs. (3.11a, b) also clarifies a situation described by Parker (1980): the best fit to a set of $M$ complex measured impedances by an expansion (3.10) is obtained when using quadratic programming. This yields a representation with at most $N=2M$ terms. In the case $N>M$ (which may occur at least for small $M$), the expansion (3.10) would require more constants than available independent data. The above representation theorem overcomes this unsatisfactory situation by compressing Eqs. (3.10) to (3.11a) or (3.11b) with exactly $2M$ constants. It the quadratic programming procedure requires $N\geqq M$ terms, the best fitting model is nonunique.

For a given representation (3.10), the condensed versions (3.11a, b) can be obtained as follows: for model I, one first either has to solve the $M$-dimensional nonlinear system (B-13) for the $M$ constants $B_m$, $m=1,\dots,M$, or one determines $B_m$ alternatively as the $M$ roots of the polynomial (B-9) with $K=M$, $q_k^{(i)}\equiv q_k$, and $q_M=1$, where the coefficients $q_k$, $k=1,\dots,M-1$ are the solution of the linear system (B-8b). With the knowledge of $B_m$ the constants $A_m$ (or $G_m$) are immediately obtained from (B-16) or (B-18). Similarly, for model II the constants $\bar{B}_m$, $m=1,\dots,M-1$, are obtained, for instance, as the solution of the first $M-1$ equations of the system (B-22) (note $b_1\geqq\bar{B}_m\geqq b_N$); $\bar{A}_0$ then follows from the $M$-th equation of (B-22) or from (B-24), and finally $\bar{A}_m$ (or $\bar{G}_m$) is given by (B-25, 26). For the solution of the various systems of nonlinear equations considered in this paper, Brown's algorithm turned out to be extremely useful, as it does not require the provision of partial derivatives. A FORTRAN program is published in Brown (1973). After the determination of the constants in Eqs. (3.11a, b), the parameters of the conductivity models are found on using the stable Rutishauser algorithm as described by Parker and Whaler (1981).

The above considerations refer to theoretical or synthetic data, for which the existence of representations (3.8) or (3.10) is granted. As mentioned above, real data can be approximated by an expansion (3.10) by quadratic programming. However, the construction of extremal models for the "cleaned" data is meaningful only for $N\geqq M$, since for $N<M$ those modified data can be interpreted by only one model.

### *3.3 General properties of the extremal models for $S(z_2)$*

In the absence of a priori constraints, the extremal models for $S(z_2)$ [Eq. (3.1)] consist of a sequence of thin sheets. The necessary extremal conditions (2.18) provide no information about the required number of sheets as a function of both $z_2$ and the number $M$ of frequencies. However, the extremal properties of models I and II considered in the previous section give the first hint. Let $S_{\max}(z_2)$ denote the upper bound of $S(z_2)$ and let $\bar{z}_\infty=\min z_\infty=\sum(A_m/B_m)$. Then the extremal models for both $S_{\max}(+0)$ and $S_{\max}(\bar{z}_\infty)$ are given by the $(M+1)$-sheet model I [extremal properties a) and b)]. Similarly, let $S_{\min}(z_2)$ signify the lower bound of $S(z_2)$ and $\bar{z}_0=\max z_0=\bar{A}_0$. Then $S_{\min}(z_2)=0$ for $z_2\leqq\bar{z}_0$ and the $M$-sheet model II is the extremal for both $S_{\min}(\bar{z}_0)$ and $S_{\min}(\infty)$ [extremal properties c) and d)]. Thus, $S_{\max}(z_2)$ and $S_{\min}(z_2)$ have models I and II, respectively, both at the beginning and end. Although it has not been proved generally, numerical experiments have shown that $S_{\max}(S_{\min})$ returns to model I (II) also at intermediate depths $z_2=\zeta_k+0$ ($z_2=\zeta_k-0$), where $\zeta_k$ is the position of a thin sheet in model I (II). Hence these models form the backbone in the evolution of the extremal models for $S_{\max}$ and $S_{\min}$ as a function of $z_2$.

To study the continuous deformation of the extremal models for varying $z_2$, the necessary condition (2.18) is discussed in more detail. In the unconstrained case the sections with $\sigma(z)>0$, implying $D(z)=0$, shrink to one point. This means that $D(z)$ must be either identically zero in the neighborhood of this point or it must show a "double zero" at the position $z=\zeta_k$ of a thin sheet *not coinciding with* $z=z_2$. Since $D(z)$ may have a discontinuous slope at $z=\zeta_k$, the necessary conditions demand

$$D(\zeta_k)=0,\qquad D'(\zeta_k-0)+D'(\zeta_k+0)=0, \tag{3.14a, b}$$

or using (2.16) and (3.7)

$$w(\zeta_k)+\operatorname{Re}\sum_{j=1}^{M}\lambda_j F_j(\zeta_k)=0, \tag{3.15a}$$

$$\operatorname{Re}\sum_{j=1}^{M}\lambda_j \bar{F}_j'(\zeta_k)=0 \tag{3.15b}$$

with $w(z)$ defined in (2.6b). Multiplying (3.15b) by $\tau_k$, the conditions (3.15a, b) are, on account of (3.6a–c), equivalent to

$$\operatorname{Re}\sum_{j=1}^{M}\lambda_j\frac{\partial c_j[\sigma]}{\partial\tau_k}=-w(\zeta_k), \tag{3.16a}$$

$$\operatorname{Re}\sum_{j=1}^{M}\lambda_j\frac{\partial c_j[\sigma]}{\partial\zeta_k}=0. \tag{3.16b}$$

Assuming a model with $K$ thin sheets, the condition (3.16b) also holds for an ultimate perfect conductor $\tau_K = \infty$ at $z=\zeta_K$, where $F_j(\zeta_K)=0=F_j'(\zeta_K-0)$, but

$$\lim_{\tau_K\to\infty} \tfrac{1}{2}\tau_K F_j'(\zeta_K-0)=\frac{\partial c_j[\sigma]}{\partial \zeta_K}=[f_j'(\zeta_K-0)]^2+0.$$

Now it is shown that the extremal model for $S_{\max}(z_2)$ always has a conducting sheet at $z_2-0$, which is just included in the range of integration, whereas $S_{\min}(z_2)$ has a conducting sheet at $z_2+0$, which is just excluded. It is assumed that $z_2$ lies between sheet $p-1$ and sheet $p$, i.e., $\zeta_{p-1}<z_2<\zeta_p$. In between, sheets $D(z)$ can vary at most as a second degree polynomial since $f_j(z)$ is a linear function in $z$. The discontinuity of $w(z)$ between $\zeta_{p-1}$ and $\zeta_p$ introduces in this range in addition a discontinuity in $D(z)$, but not in $D'(z)$:

$$D(z_2+0)-D(z_2-0)=\begin{cases}+1 & \text{for } S_{\max}(z_2)\\ -1 & \text{for } S_{\min}(z_2)\end{cases}, \qquad (3.17)$$

$$D'(z_2+0)-D'(z_2-0)=0. \qquad (3.18)$$

First, it is shown that the conditions (3.14a, b) in connection with the quadratic variation of $D(z)$ lead to the conclusion that $D(z)\equiv 0$ for $z\geqq\zeta_p$. From $f_j(z)=$const. for $z\geqq\zeta_K$ and $D(\zeta_K)=0$ follows $D(z)\equiv 0$ for $z\geqq\zeta_K$. With $D'(\zeta_K+0)=0$ it is inferred from Eq. (3.14b) that also $D'(\zeta_K-0)=0$. Hence for $p<K$ we have $D(z) = A_K(z-\zeta_K)^2$ in $\zeta_{K-1}\leqq z\leqq\zeta_K$, where $D(z)\geqq 0$ implies $A_K\geqq 0$. However, $A_K=0$, since $D(\zeta_{K-1})=0$ on account of Eq. (3.14a). Therefore, $D(z)\equiv 0$ in $\zeta_{K-1}\leqq z\leqq\zeta_K$. Repeating the arguments, it is found that $D(z)\equiv 0$ for $z\geqq\zeta_p$. In $\zeta_p>z\geqq z_2+0$ we again have $D(z)=A_p(z-\zeta_p)^2$, $A_p\geqq 0$. With reference to Eq. (3.18), $D'(z)$ is a continuous linear function in $\zeta_{p-1}\leqq z\leqq\zeta_p$ with $D'(\zeta_p-0)=0$, $D''(\zeta_p-0)\geqq 0$, implying $D'(\zeta_{p-1}+0)\leqq 0$. On the other hand, if $\zeta_{p-1}+0<z_2<\zeta_p-0$, then the two conditions $D(\zeta_{p-1}) =0$ and $D(z)\geqq 0$ would require $D'(\zeta_{p-1}+0)\geqq 0$. This does not contradict the preceding result only if $D'(\zeta_{p-1}+0)=0$, implying $A_p=0$ and $D(z)\equiv 0$ in $\zeta_{p-1}\leqq z\leqq\zeta_p$ [because of the continuity of $D'(z)$]. The condition (3.17), however, requires that $D(z)\not\equiv 0$ in this interval. The remedy is to take either $z_2=\zeta_{p-1}+0$ or $z_2 =\zeta_p-0$. In this case a thin sheet lies at the *preassigned* depth $z_2\pm 0$, which is no longer a freely variable parameter and hence is not to be included in the necessary conditions (3.14b)–(3.16b). In view of Eq. (3.17), the case $z_2=\zeta_{p-1}+0$ applies to $S_{\max}$ with

$$D(z_2-0)=D(\zeta_{p-1})=0, \qquad D(z_2+0)=1, \qquad (3.19\text{a})$$

and the case $z_2=\zeta_p-0$ pertains to $S_{\min}$:

$$D(z_2+0)=D(\zeta_p)=0, \qquad D(z_2-0)=1. \qquad (3.19\text{b})$$

Since the evolution of the extremal models for varying $z_2$ is quite involved in the general case, it will be studied in detail only by two relatively simple examples for one and two frequencies.

### 3.4 Extremal models for one frequency

The data for the frequency $\omega_1=:\omega$ is $c_1=:c$ with

$$c=g-ih=|c|e^{-i\psi}, \qquad (3.20)$$

where $|c|$ is related to the apparent resistivity $\rho_a$ and apparent conductivity $\sigma_a$ by

$$\rho_a=\omega\mu_0|c|^2, \quad \sigma_a=1/\rho_a, \qquad (3.21)$$

and $\psi$ is the complement to the phase $\varphi$ between the electric and magnetic field, $\varphi+\psi=90°$. The data is consistent with a $1D$ model if $g\geqq 0$, $h\geqq 0$, or equivalently $0\leqq\psi\leqq 90°$. The results of the last section have already shed some light on the structure of the extremal models. The associated models I and II [Eq. (3.11a, b)] using the notation of Sects. 3.1 and 3.2 are

$$\text{I:}\ c[\sigma]=\frac{A_1}{B_1+i\omega}=\frac{\zeta_2}{1+i\omega\mu_0\tau_1\zeta_2}, \qquad (3.22\text{a})$$

$$\text{II:}\ c[\sigma]=\bar{A}_0+\frac{\bar{A}_1}{i\omega}=\zeta_1+\frac{1}{i\omega\mu_0\tau_1}. \qquad (3.22\text{b})$$

Equating with Eq. (3.20), it is found that model I consists of a thin sheet with conductance $\tau_1=|c|\sigma_a\sin\psi$ at $z=0$ and a second sheet with $\tau_2=\infty$ at $z_\infty=|c|\sec\psi$, whereas model II consists of a single sheet $\tau_1= |c|\sigma_a/\sin\psi$ at $z_0=|c|\cos\psi$. Hence,

$$S_{\max}(+0)=|c|\sigma_a\sin\psi,$$
$$S_{\max}(z_2)=\infty,\ z_2\geqq|c|\sec\psi, \qquad (3.23\text{a})$$

$$S_{\min}(\infty)=|c|\sigma_a/\sin\psi,$$
$$S_{\min}(z_2)=0,\ z_2\leqq|c|\cos\psi. \qquad (3.23\text{b})$$

The models of the start and end are identical, with the difference, however, that at the end the (lower) sheet is included in $S$. Now the evolution of the models between these limits has to be studied. Starting with $S_{\max}$, it is assumed that the extremal model for $z_2>0$ evolves from that of $z_2=+0$ by moving the surface sheet to $\zeta_1=z_2-0>0$. Then also the second sheet with $\tau_2=\infty$ will move. The two free parameters of the model are $\tau_1$ and $\zeta_2$, whereas $\zeta_1$ and $\tau_2$ are preassigned. From Eqs. (2.7a) and (3.16a, b) results the system

$$c[\sigma]=c, \qquad (3.24\text{a})$$

$$\mathrm{Re}\left\{\lambda\frac{\partial c[\sigma]}{\partial\tau_1}\right\}=1, \qquad (3.24\text{b})$$

$$\mathrm{Re}\left\{\lambda\frac{\partial c[\sigma]}{\partial\zeta_2}\right\}=0 \qquad (3.24\text{c})$$

($\lambda_1=:\lambda$), where the partial derivatives of $c[\sigma]$ are determined from (3.6a–c). The system (3.24a–c) consists of four real equations for the four real unknowns $\tau_1$, $\zeta_2$, $\mathrm{Re}\,\lambda$, and $\mathrm{Im}\,\lambda$. In practice, first Eq. (3.24a) is solved for $\tau_1$ and $\zeta_2$ to obtain $S_{\max}(z_2)=\tau_1$, and then Eq. (3.34b, c) is solved for the sensitivity measure $\lambda$, which is required, for instance, in the discriminant function (2.16)

$$D(z)=w(z)+\mathrm{Re}\,\{\lambda F(z)\}$$

with $F(z):=F_1(z)$, as defined in Eq. (2.14). This nonnegative function has to vanish at $z=\zeta_1$ and $z=\zeta_2$, where $D(\zeta_1)=0$ is equivalent to Eq. (3.24b) and $D(\zeta_2) =0$ is satisfied because of $F(\zeta_2)=0$. With the present two-sheet model the condition $D(z)\geqq 0$ can be satisfied only for sufficiently small $z_2$. This is a consequence of $D(\zeta_1)=D(z_2-0)=0$ and the fact that $D(z)$ is a second-degree polynomial in $0\leqq z\leqq z_2$, which for some limiting value $z_2 = z_a$ vanishes at $z=0$ and thus signals the emergence of a third sheet at $z=0$. To determine $z_a$, the system (3.24a–c) is augmented by the condition $D(0)=0$. This condition and (3.24b, c) are linear in the two unknowns $\operatorname{Re}\lambda$ and $\operatorname{Im}\lambda$ and are compatible only if linearly dependent. Using $F(\zeta_1)=\partial c/\partial\tau_1$, the compatibility condition is

$$\operatorname{Im}\left\{[F(\zeta_1)-F(0)]\Big/\frac{\partial c[\sigma]}{\partial\zeta_2}\right\}=0.$$

Expressing $F$ and $c[\sigma]$ in terms of $\tau_1$, $\zeta_1(=z_2-0)$, and $\zeta_2$, this condition reads

$$(\zeta_1-\zeta_2)^2(1+\omega^2\mu_0^2\tau_1^2\zeta_1^2)=\zeta_2^2,$$

and writing $\tau_1$ and $\zeta_2$ in terms of the data, we end up with a cubic equation for $z_a=\zeta_1$ as limiting value of $z_2$:

$$z_a^3-4gz_a^2+(2g^2+3|c|^2)z_a-2g|c|^2=0. \tag{3.25}$$

Of interest is the root $z_a$ in $0\leqq z_a\leqq g=|c|\cos\psi$.

Renumbering the sheet parameters in the three-sheet problem, the determination of $S_{\max}(z_2)=\tau_1+\tau_2$ for $z_2>z_a$ requires the determination of $\tau_1$, $\tau_2$, and $\zeta_3$ from the set of equations

$$c[\sigma]=c, \tag{3.26a}$$

$$\operatorname{Re}\left\{\lambda\frac{\partial c[\sigma]}{\partial\tau_1}\right\}=1, \tag{3.26b}$$

$$\operatorname{Re}\left\{\lambda\frac{\partial c[\sigma]}{\partial\tau_2}\right\}=1, \tag{3.26c}$$

$$\operatorname{Re}\left\{\lambda\frac{\partial c[\sigma]}{\partial\zeta_3}\right\}=0. \tag{3.26d}$$

In practice, first $\tau_1$, $\tau_2$, and $\zeta_3$ are computed from (3.26a) and the compatibility condition

$$\operatorname{Im}\left\{\left[\frac{\partial c[\sigma]}{\partial\tau_2}-\frac{\partial c[\sigma]}{\partial\tau_1}\right]\Big/\frac{\partial c[\sigma]}{\partial\zeta_3}\right\}=0,$$

and $\lambda$ is obtained in turn from two of the three equations (3.26b–d).

With the emergence of the third sheet, the perfectly conducting ultimate sheet, which was first moving downwards, is moving upwards again and merges for $z_2\to z_\infty=|c|\sec\psi$ with the sheet at $z_2-0$, which is getting increasingly conductive. The conductance of the surface sheet has meantime increased to $|c|\sigma_a\sin\psi$, and we return for $z_2=z_\infty$ to the conductivity model for $z_2=+0$.

The extremal models for $S_{\min}(z_2)$ evolve similarly. As mentioned earlier, $S_{\min}(z_2)=0$ for $z_2\leqq g=|c|\cos\psi$. For $z_2>g$ we try a model consisting of a surface sheet of conductance $\tau_1$ at $z=\zeta_1=0$ and a second sheet of conductance $\tau_2$ at $z=\zeta_2=z_2+0$. The unknowns are $\tau_1$ and $\tau_2$. The system of equations analogous to (3.24a–c) is

$$c[\sigma]=c, \tag{3.27a}$$

$$\operatorname{Re}\left\{\lambda\frac{\partial c[\sigma]}{\partial\tau_1}\right\}=-1, \tag{3.27b}$$

$$\operatorname{Re}\left\{\lambda\frac{\partial c[\sigma]}{\partial\tau_2}\right\}=0. \tag{3.27c}$$

Again, Eq. (3.27a) is sufficient to determine $\tau_1$ and $\tau_2$. The two-sheet model with the fixed surface sheet has to be modified, when $\zeta_1$ can also be considered as a variable, i.e. if, in addition to Eq. (3.27a–c), the following holds

$$\operatorname{Re}\left\{\lambda\frac{\partial c[\sigma]}{\partial\zeta_1}\bigg|_{\zeta_1=0}\right\}=0. \tag{3.27d}$$

The augmented system (3.27a–d) allows the determination of the limiting value $z_2=z_i$, where the surface sheet starts moving. The condition of linear dependence of (3.27b–d) leads to

$$\operatorname{Im}\left\{\frac{\partial c[\sigma]}{\partial\tau_2}\Big/\frac{\partial c[\sigma]}{\partial\zeta_1}\bigg|_{\zeta_1=0}\right\}=0,$$

or

$$\tau_1+2\tau_2=\omega^2\mu_0^2\tau_1\tau_2^2\zeta_2^2.$$

The expression of $\tau_1$ and $\tau_2$ in terms of the data then yields again a cubic equation for $\zeta_2=z_i$:

$$4g^2z_i^3-4g(|c|^2-g^2)z_i^2 \\ +|c|^2(|c|^2-4g^2)z_i-|c|^4g=0. \tag{3.28}$$

Of interest is the solution $z_i\geqq g$ with $z_i\to|c|^2/(2g)$ for $z_i\to\infty$. For $z_2>z_i$ the system (3.27a–c) is augmented by

$$\operatorname{Re}\left\{\lambda\frac{\partial c[\sigma]}{\partial\zeta_1}\right\}=0$$

and the unknowns $\tau_1,\tau_2$, and $\zeta_1$ are determined from Eq. (3.27a) and

$$\operatorname{Im}\left\{\frac{\partial c[\sigma]}{\partial\tau_2}\Big/\frac{\partial c[\sigma]}{\partial\zeta_1}\right\}=0.$$

The surface sheet, starting moving for $z_2=z_i$, approaches $z=g$ for $z_2\to\infty$ and attains the conductance $\tau_1=|c|\sigma_a/\sin\psi$. In this limit the lower sheet disappears at infinity, and we return to the starting one-sheet model.

Figure 1 shows $z_a(\psi)$, $z_i(\psi)$, and $z_\infty(\psi)$. It also sketches the type of extremal models for the various ranges of $z_2$. The depth $z^*=g=|c|\cos\psi$ is the "center of gravity" of the induced currents. Unless there is only one sheet, conductors must be present both above and below $z^*$. The extremal models are not unique for $S_{\max}$ in the range $z_2>z_\infty$ ($S_{\max}=\infty$) and for $S_{\min}$ in the range $0\leqq z_2<z_0=g$ ($S_{\min}=0$). The *position* of conducting sheets for $\psi=45°$ is depicted in the left part of Fig. 6 as function of $z_2$.

Figure 2 displays the curves bounding $S(z_2)$ for different phases $\psi$. $S$ is normalized by the conductance $|c|\sigma_a=1/(\omega\mu_0|c|)$ [Eq. (3.21)]. All models compatible with the two-data problem must fall into the shaded areas. These areas get narrow both for $\psi\to0°$ and $\psi\to90°$, reflecting the fact that these two limiting phases can be interpreted by one model only, consisting, respectively, of a perfect conductor at $z=|c|$ and a thin sheet of conductance $|c|\sigma_a$ at $z=0$. The limiting values of $S_{\max}$ and $S_{\min}$ as a function of $\psi$ are given in Eq. (3.23a, b).

As a particular feature of Fig. 2, note that the shaded areas for $\psi$ and $90°-\psi$ are mirror images obtained

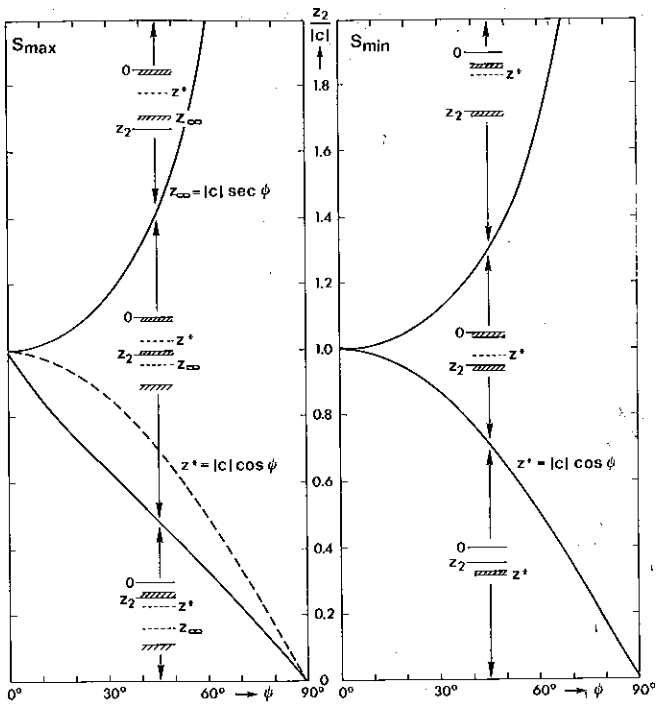


**Fig. 1.** The different types of extremal models in the unconstrained one-frequency case as function of the phase $\psi$. In $S_{max}$ a surface sheet emerges for $z_2 = z_a(\psi)$ (*lower solid curve at left*) and in $S_{min}$ the surface sheet is detached for $z_2 = z_i(\psi)$ (*upper curve at right*)

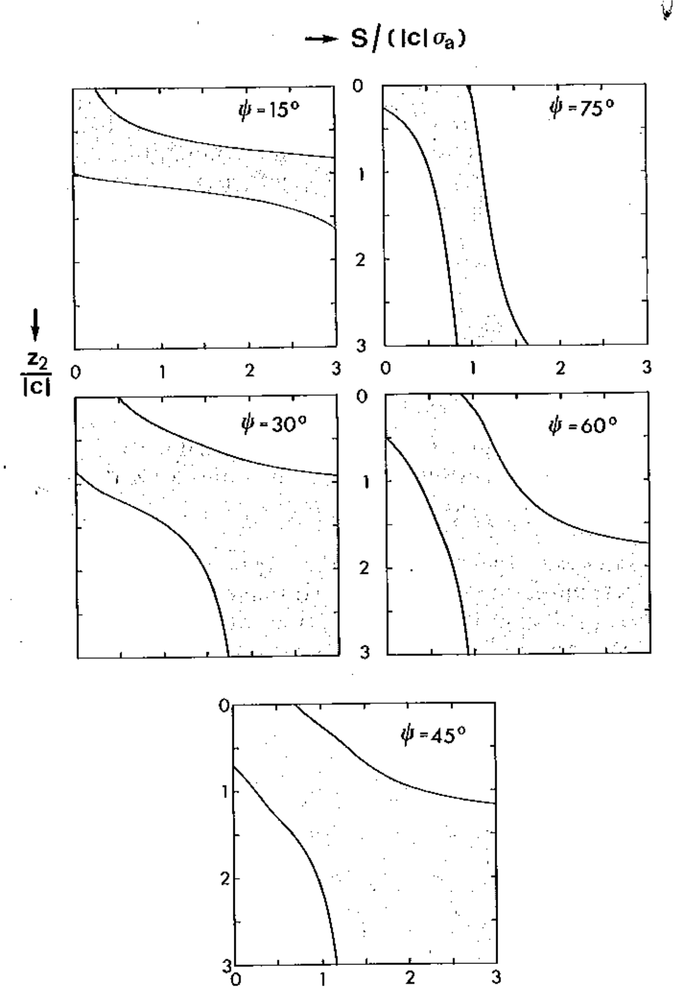


**Fig. 2.** The bounds for $S(z_2)$ in the unconstrained one-frequency case for different phases $\psi$. The mirror symmetry of the *shaded* domains for $\psi$ and $90° - \psi$ is explained in the text

by reflection at the main diagonal. This is an expression of the duality transformation (Weidelt, 1972), which transforms Eq. (2.2) by means of

$$\bar{z} := \int_0^z \sigma(\zeta)/\sigma_0 \, d\zeta, \quad \bar{\sigma}(\bar{z}) := \sigma_0^2/\sigma(z), \tag{3.29a, b}$$

$$\bar{f}(\bar{z}) := f'(z) \tag{3.29c}$$

into

$$\bar{f}''(\bar{z}) = i\omega\mu_0 \bar{\sigma}(\bar{z}) \bar{f}(\bar{z}) \tag{3.30}$$

with

$$\bar{c}(\omega) = -\bar{f}(0)/\bar{f}'(0) = 1/[i\omega\mu_0\sigma_0 c(\omega)], \tag{3.31}$$

where $\sigma_0 > 0$ is an arbitrary reference conductivity. Equations (3.29a, b) and (3.31) imply

$$S(z) = \sigma_0 \bar{z}, \quad \bar{S}(\bar{z}) = \sigma_0 z, \quad \psi + \bar{\psi} = 90°$$

and admit the following interpretation. When determining for given $z_2$ and $\psi$ the bounds $S_{max}(z_2)$ and $S_{min}(z_2)$, one automatically also solves the dual problem consisting in determining for $\bar{\psi} = 90° - \psi$ and $\bar{S}_2 = \sigma_0 z_2$ the depth bounds $\bar{z}_{max}(\bar{S}_2)$ and $\bar{z}_{min}(\bar{S}_2)$, to which $\bar{\sigma}(\bar{z})$ has to be integrated to reach the given conductance $\bar{S}_2$ under the most adverse and favorable conditions. The congruence of the shaded areas results from the particular scaling on exploiting $|c|\sigma_a = |\bar{c}|\sigma_0$, $|\bar{c}|\bar{\sigma}_a = |c|\sigma_0$ [Eq. (3.31)]. The symmetry between conductance and depth breaks down, if a priori constraints are imposed on conductivity (cf. Fig. 7).

### *3.5 Extremal models for two frequencies*

For more than one frequency various different situations may occur in the evolution of the extremal models, and the general discussion becomes cumbersome (or even impossible). For this reason, attention is confined in this section to the exemplary study of a real data set for $M=2$ frequencies, consisting of the estimates of the transfer function $c$ for the first and fourth $Sq$ harmonic for Europe as given by Schmucker (1984):

1 cpd: $c_1 = (575 - i260)$ km

4 cpd: $c_2 = (290 - i275)$ km.

By quadratic programming on using the program NNLS of Lawson and Hanson (1974) [as suggested by Parker (1980)], it is found that the data can be represented *exactly* by the series (3.10) with the maximum number of $N = 2M = 4$ terms. The condensation of this series according to Eq. (3.11a, b) then yields the two canonical models

$$\text{I:} \quad \begin{aligned} &\zeta_1 = 0, && \tau_1 = 4.09466 \cdot 10^3\,S \\ &\zeta_2 = 5.23675 \cdot 10^5\,m, && \tau_2 = 3.77586 \cdot 10^4\,S \\ &\zeta_3 = 7.83023 \cdot 10^5\,m, && \tau_3 = \infty \end{aligned}$$

$$\text{II:} \quad \begin{aligned} &\zeta_1 = 1.05947 \cdot 10^5\,m, && \tau_1 = 6.66233 \cdot 10^3\,S \\ &\zeta_2 = 6.99673 \cdot 10^5\,m, && \tau_2 = 1.01835 \cdot 10^5\,S \end{aligned}$$

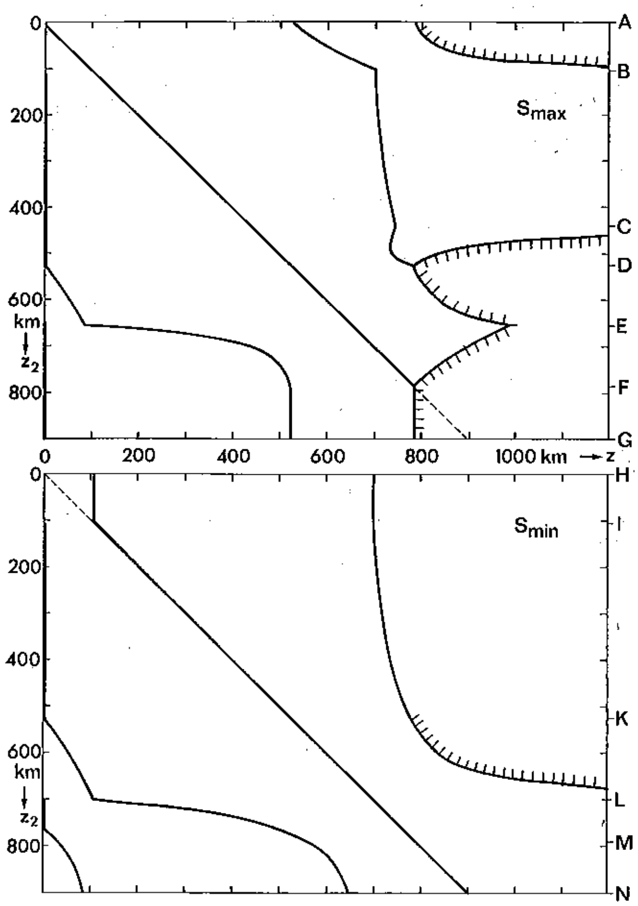


Fig. 3. The position $z$ of conducting sheets as function of $z_2$ in the extremal models for the unconstrained two-frequency problem (first and fourth $Sq$ harmonic)

(giving for a possible check of the algorithm three to four more digits than warranted by the accuracy of the data). $S_{max}(z_2)$ has model I not only at the start and end, but returns to it also at the intermediate depth $z_2 \simeq 524$ km. Similarly, $S_{min}(z_2)$ also returns to model II at $z_2 \simeq 700$ km. The position $z$ of conducting sheets (abscissa) as a function of $z_2$ (ordinate) is shown in Fig. 3 for $S_{max}$ and $S_{min}$. The ticks mark perfectly conducting sheets. This figure provides an idea of the nonlinearities in the problem by showing emerging, coalescing, disappearing, and reappearing sheets.

The continuous deformation of the start model to an identical end model is performed, on the one hand, by the sheets emerging at $z=0$ (level $B$, $E$, $I$, and $L$) and getting detached at $D$, $K$, and $M$, and on the other by the lower sheets either coalescing at $D$ and $F$ with the ultimate perfect conductor ($S_{max}$), or moving at $L$ and below $N$ to infinity ($S_{min}$).

Model I is realized at $A$, $D$, $K$, and below $F$, whereas model II occurs at $B$, $I$, $L$, and below $N$ for $z_2 \to \infty$. The models for $S_{max}$ in the ranges $\overline{BC}$ and $\overline{DE}$ are identical with those of $S_{min}$ in the same range of $z_2$; $S_{max}$ and $S_{min}$ differ only by the conductance of the sheet at $z_2$. In the missing range $\overline{CD}$ all necessary conditions imposed on $S_{max}$ can be satisfied on taking the same model as for $S_{min}$, but it turns out that choosing the four-sheet model for $S_{max}$ with the reappearing perfect conductor produces in this range slightly greater values. This underlines the fact that the conditions derived in Sect. 2 are necessary but not sufficient.

Figure 4 displays the resulting bounds for the two frequencies, along with the bounds obtained by each frequency separately. In the present example, joint consideration of the two frequencies improves spectacularly the lower bound on $S$, whereas the upper bound curve deviates only slightly from the curve consisting of the smaller of the values of $S_{max}$ obtained by single-frequency interpretation. At level $z_2 = \zeta_2$ of model II, the values of $S_{min}$ for 1 cpd and 1&4 cpd do not appear to be strictly equal, but differ only by 0.01%. The marks at the right margin denote the depth of the shallowest perfect conductor, moving from 551 km for 4 cpd to 692 km for 1 cpd and to 783 km for 1 & 4 cpd.

Finally, it is noted that at the distinguished levels $z_2 \simeq 106$, 524, and 700 km, where the slope of the bounding curves changes discontinuously, the Lag-

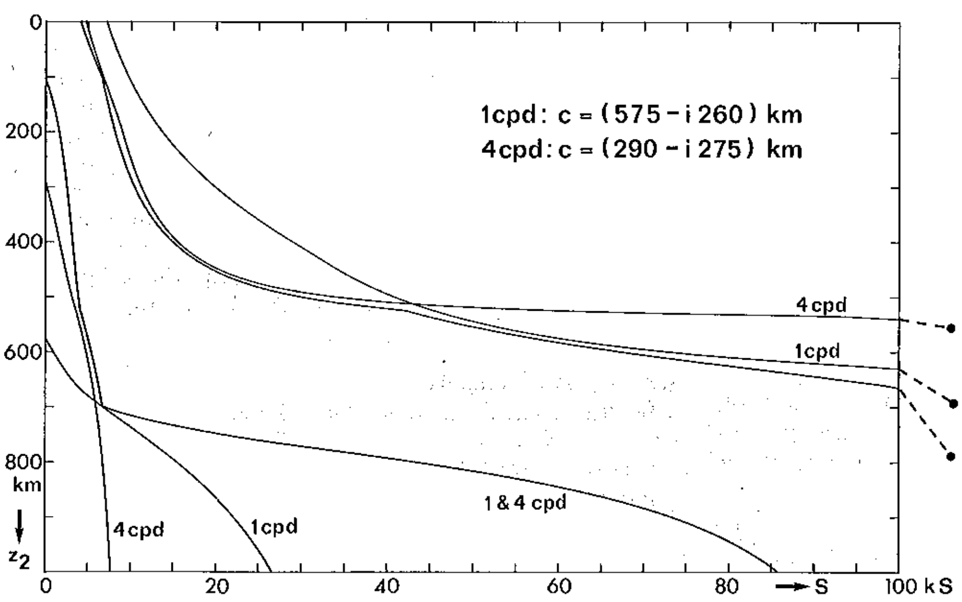


Fig. 4. Bounds for $S(z_2)$ in the unconstrained two-frequency problem. All models fitting these data must fall into the *shaded* area. The joint consideration of 1 and 4 cpd considerably improves the bound for $S_{min}$ and shows that all models must have a good conductor not deeper than 700-800 km

rangian multipliers $\lambda_1$ and $\lambda_2$ are also discontinuous, meaning that near these levels the relation (2.10) for an estimate of the influence of data errors has to be applied with caution (cf. also case C1 in Sect. 3.6).

### 3.6 *Extremal models for many frequencies*

As a basic limitation of this study, it is assumed that there is a $1D$ model, which exactly fits the data set. This restriction may be dropped in subsequent work, where the equality constraints (2.7a) are replaced by inequality constraints that demand only a fit of the data within a suitable multiple of the standard deviation. With the present tools, however, there are two approximate ways to handle inconsistent data:

a) The $1D$ information (3.10) is extracted by quadratic programming; the cleaned data allow a reasonable construction of extremal models only if the number $M$ of frequencies does not exceed the number $N$ of terms, since for $M>N$ only one model exists.

b) Extremal models are constructed for different consistent subsets of the data, and the bounds on $S(z_2)$ for the whole set are estimated by taking the greatest of the lower bounds for each $z_2$ and the smallest of the upper bounds. In the simplest case a consistent subset comprises the data for just one frequency, requiring only $\operatorname{Re} c \geqq 0$, $\operatorname{Im} c \leqq 0$.

Generalizing the experience gained from a small number of frequencies, it appears that in the $M$-frequency case the extremal models belong to one of the six categories:

A1: The model consists of $M+1$ thin sheets with $\tau_{M+1}=\infty$ and with one sheet fixed at depth $z_2$. There remain $2M$ free model parameters, which can be determined from the $2M$ real data. If required, the $M$-complex multipliers $\lambda_j$ are obtained by solving the linear system of order $2M$ resulting from the necessary conditions (3.16a, b) for the $2M$ free model parameters (examples in Fig. 3: $\overline{AB}$, $\overline{DE}$, $\overline{KL}$).

A2: This case differs from A1 only in preassigning $\zeta_1=0$ rather than $\tau_{M+1}=\infty$ (examples: $\overline{BC}$, $\overline{IK}$, $\overline{LM}$).

B1: $M+2$ sheets with preassigned $\zeta_1=0$, $\tau_{M+2}=\infty$, and one sheet at fixed depth $z_2$. There remain $2M+1$ free model parameters, for which there are $2M+1$ equations of type (3.16a, b), linear in the $2M$ real quantities $\operatorname{Re}\lambda_j$ and $\operatorname{Im}\lambda_j$. As a compatibility condition, the determinant of order $2M+1$ formed by the matrix of the linear system and the right-hand side of (3.16a, b) as $(2M+1)st$ column has to vanish. This equation in connection with the $2M$ data furnishes $2M+1$ nonlinear equations for the $2M+1$ free-model parameters. If required, the multipliers $\lambda_j$ can finally be obtained by $2M$ of the linear equations (omitting an equation with the right-hand side vanishing). Examples are $\overline{CD}$, $\overline{EF}$.

B2: $M+1$ sheets of finite conductance with one sheet fixed at $z=z_2$. There are again $2M+1$ free-model parameters, which are determined in analogy to B1 (example: $\overline{MN}$).

C1: $M+1$ sheets with $\zeta_1=0$, $\tau_{M+1}=\infty$ (=canonical model I), $z_2$ happens to coincide with the position of one of the sheets. The $2M$-model parameters (including $z_2$) can be determined from the $2M$ data. However, the multipliers $\lambda_j$ remain undefined, since Eqs. (3.16a, b) yield only $2M-1$ real equations ($z_2$ fixed!) for the $M$ complex $\lambda_j$. In fact, the $\lambda_j$ are discontinuous for these special values of $z_2$, yielding different sets for slightly smaller and greater $z_2$ (examples: $A$, $D$, $F$, $K$).

C2: $M$ sheets of finite conductance (=canonical model II), $z_2$ coincides with one of the sheets (cf. C1 for further discussion; examples: $B$, $I$, $L$).

The models A1 and A2, B1 and B2, C1 and C2 are dual in the sense of Sect. 3.2.

The model type for varying $z_2$ may have to be changed for the following reasons:

a) The system of nonlinear equations no longer has a solution (e.g., because the deepest perfectly conducting sheet disappears or reappears at infinite depth or merges with another sheet, or the conductance of the deepest sheet increases from finite values to infinity).

b) A surface sheet emerges. According to Eqs. (3.14a), (2.14), and (2.3), the condition is

$$D(0)=w(0)-\operatorname{Re}\sum_{j=1}^{M} i\omega_j\mu_0\lambda_j c_j^2=0,$$

whereas $D(0)>0$ in the absence of a surface sheet.

c) The surface sheet becomes detached and moves downwards. This happens when $\zeta_1$ becomes a freely varying parameter, implying according to (3.14b), (2.14), (2.3), and (3.2) that

$$D'(-0)+D'(+0)=\operatorname{Re}\sum_{j=1}^{M} 2i\omega_j\mu_0 c_j\lambda_j(2-i\omega_j\mu_0\tau_1 c_j)=0.$$

This section concludes with an example for approximate extremal models from an inconsistent data set. We choose the COPROD data of Jones (1980), which have been inverted by different authors using a variety of techniques. The shaded area in Fig. 5 was determined by the approximate method b) from 11 consistent subsets comprising a single frequency. The figure also displays as $S(z_2)$-curves the various results of inversion. These models freely use the space allotted them and occasionally even transgress it because of the approximate nature of bounds and models. This example shows that the approximate method b), which for consistent data tends to produce conservative bounds (cf. $S_{min}$ in Fig. 4), can even yield too narrow bounds for inconsistent data, where the range of acceptable models is broader because in fitting the data different frequencies (or frequency bands) can be emphasized. Also, inconsistencies in the data may lead to unreasonable restrictions in the feasible (shaded) area. For this reason the four longest periods contained in the COPROD data have been omitted when constructing the bounds.

## 4. Extremal models for the constrained conductance function

Section 3 was devoted to the unconstrained extremal models with $\sigma_-(z)\equiv 0$, $\sigma_+(z)\equiv\infty$. In this section we shall consider as a simple example for constrained extremal models the one-frequency problem of Sect. 3.4, where now the range of admitted conductivities is

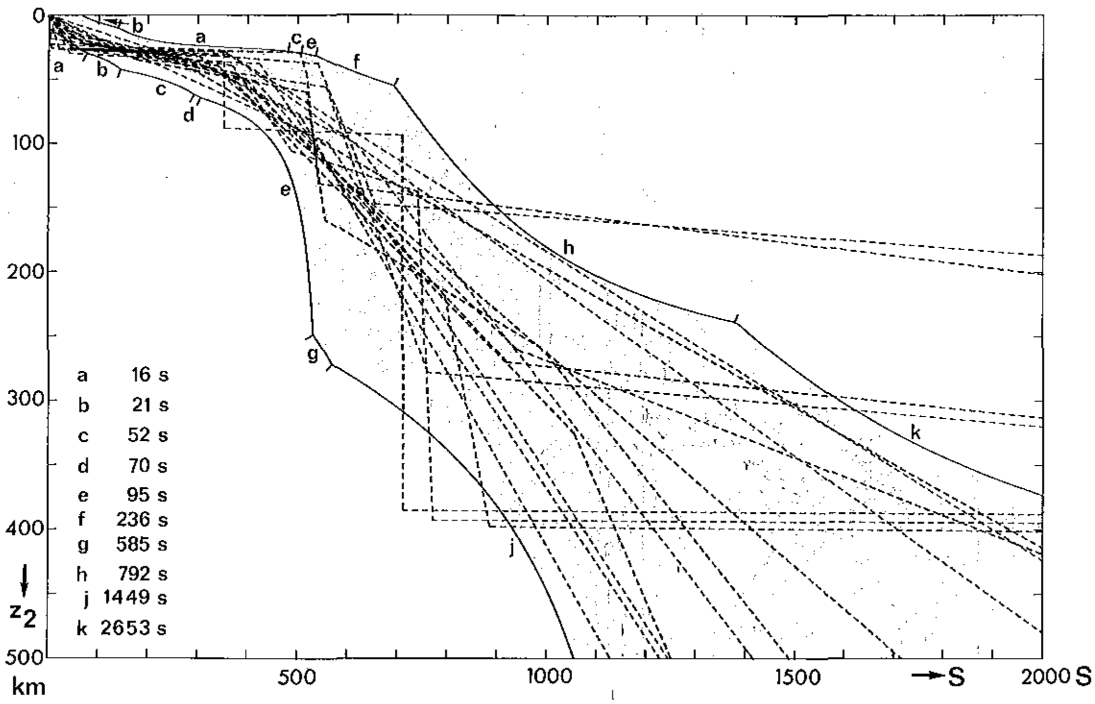


**Fig. 5.** Approximate bounds on $S(z_2)$ as derived from the 11 shortest periods of the COPROD data; only the 10 periods listed have contributed to the bounds. In general, longer periods should be binding at greater depth. Due to inconsistent data the longer period of 21 s (b) is bounding $S_{max}$ at shallower depth than the shorter period of 16 s (a). Also displayed as $S(z_2)$ curves are the results of the various interpreters

bounded by $\sigma_+(z) \equiv \sigma_+$, where $\sigma_+$ is a positive constant. In particular, the structure of the extremal models is studied when assigning to $\sigma_+$ a varying multiple $\alpha$ of the apparent conductivity $\sigma_a$ [cf. (3.21)], i.e., $\sigma_+ = \alpha\sigma_a$. In this particular case, the extremal models consist of a sequence of uniform layers with $\sigma(z)=\sigma_+$ and insulators with $\sigma(z)=0$. According to Eq. (2.20), the necessary extremal conditions are $D(z) \geq 0$ for $\sigma(z)=0$ and $D(z) \leq 0$ for $\sigma(z)=\sigma_+$, with layer boundaries at positions where $D(z)$ changes sign.

Before considering more details, it might be useful to discuss first the structure of the extremal models as displayed in Fig. 6 for $\psi=45°$ and various values of $\alpha$. The position of the thin sheets (abscissa) as a function of $z_2$ (ordinate) in the unconstrained case $\alpha=\infty$ is shown at the left. The ticks mark again perfect conductors. The main structural units of these models are clearly discernible in the following models of constrained conductivity, where the layers with $\sigma=\sigma_+$ are shaded. As expected from experience with the unconstrained case, $S_{min}$ generally shows a conducting layer starting at $z=z_2$, which is just excluded from the range of integration, whereas $S_{max}$ in general has a conducting layer, which ends at $z_2$ and is just included. There are two notable exceptions (dashed diagonal). For sufficiently small $z_2$, the extremal models demand only that $\sigma=0$ for $S_{min}$ and $\sigma=\sigma_+$ for $S_{max}$ in $0 \leq z \leq z_2$, which can be reached in different ways. When $z_2$ exceeds a certain limit, however, there will only be one model. This first unique model is then also shown for smaller $z_2$. This situation is comprised in the extremal condition (2.20) since, in this range of $z_2$, $S_{min}$ and $S_{max}$ do not depend on the data, i.e., $\lambda=0$ [Eq. (2.10)] and $D(z)=w(z)$, which is non-negative for $S_{min}$ and non-positive for $S_{max}$. The other exception occurs for $S_{max}$ in a certain range below the point, where the two conducting layers merge into a thick conductor having $z=z_2$ as interior point. In this case $D(z_2-0)<-1$ and $D(z_2+0)=D(z_2-0)+1<0$, i.e., $D(z)$ does not change sign at $z=z_2$.

For smaller values of $\alpha$, the conducting layers necessarily become thicker, and for $\alpha=1$ the extremal models for $S_{max}$ are just uniform half-space models. Therefore, the case of $\alpha=1.1$, for which narrow non-conductive channels still occur, is considered. Due to the overshot phenomenon of the apparent resistivity curve, it is possible to construct extremal models even for $\alpha<1$, meaning that the true conductivity is smaller everywhere than the apparent conductivity. It is easily verified that for the considered phase $\psi=45°$ the smallest value of $\alpha$ is $\alpha_{min}=\tanh^2(\pi/2)=0.8412$, which corresponds to a surface layer of conductivity $\alpha_{min}\sigma_a$, thickness $(\pi|c|/\sqrt{2})$ coth $(\pi/2)=2.4221\,|c|$, and an insulator below. For the smallest possible conductivity the models for $S_{min}$ and $S_{max}$ coincide and are independent of $z_2$.

The resulting bounding curves of $S(z_2)$ for selected values of $\alpha$ (curve parameter) are shown in Fig. 7. A bounded value of $\alpha$ mostly affects $S_{max}$, whereas $S_{min}$ is only influenced for relatively small $\alpha$. The dashed lines refer to the smallest possible value of $\alpha$, for which only one model exists. For $0 \leq \psi < 45°$ it consists of a slab at finite depth, and for $45° \leq \psi \leq 90°$ it is a surface slab.

The actual construction of the extremal models is similar to that in the unconstrained case. If $\sigma_-(z)$ and $\sigma_+(z)$ are independent of $z$, the conductivity models

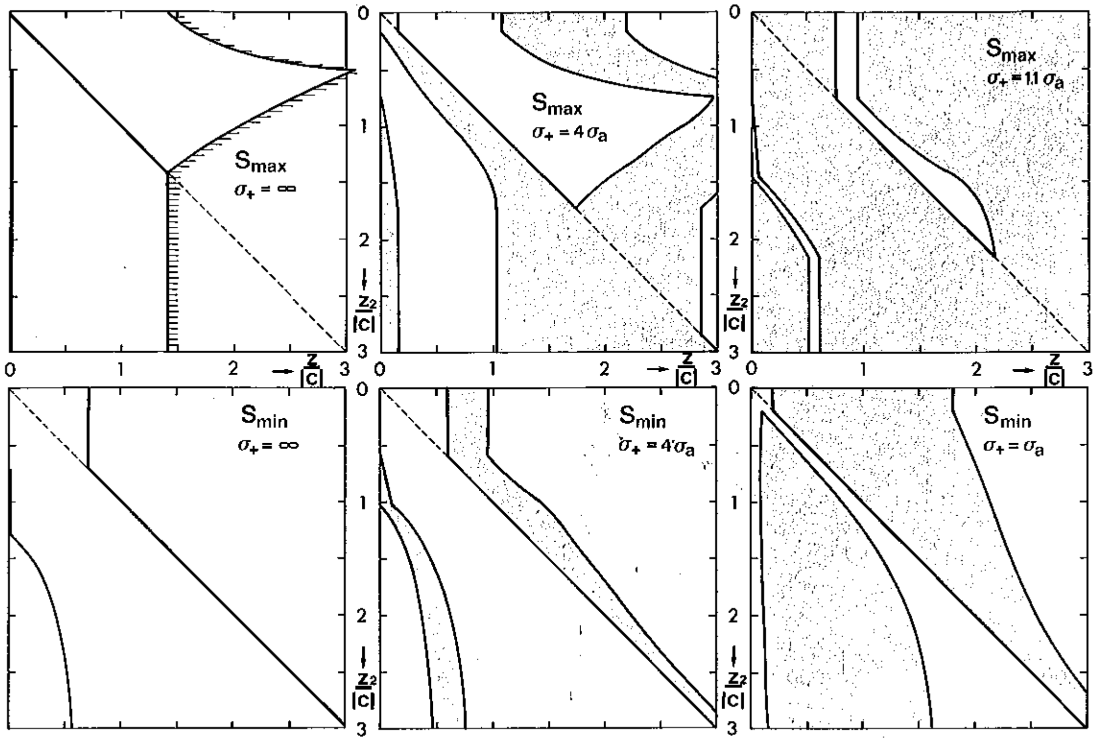


**Fig. 6.** Structure of the unconstrained (*left*) and constrained (*center and right*) one-frequency extremal models for $\psi = 45°$. For a given $z_2$ (*ordinate*) the unconstrained models are presented only by the position of the conducting thin sheets (without specifying their conductance), whereas the constrained models ($\sigma_+ < \infty$) are completely characterized by specifing the position of the conducting layers (*shaded*)

consist of a sequence of uniform layers. The pertinent formulae are briefly summarized. Let $K$ uniform layers exist, with the top at $z = \zeta_k$ ($\zeta_1 = 0$), and layer conductivities $\sigma_k$, $k = 1, \ldots, K$. With $\gamma_k^2 := i\omega\mu_0\sigma_k$ and $d_k := \zeta_{k+1} - \zeta_k$ as thickness of layer $k$, $k = 1, \ldots, K-1$, the theoretical response $c[\sigma] = c_1$ is recursively determined from

$$c_k = \frac{1}{\gamma_k}\,\frac{\gamma_k c_{k+1} + \tanh(\gamma_k \alpha d_k)}{1 + \gamma_k c_{k+1} \tanh(\gamma_k d_k)}, \qquad k = K-1, \ldots, 1 \tag{4.1}$$

starting with $c_K = 1/\gamma_K$. [Note again that in this context the subscript $k$ on $c$ refers to the level $\zeta_k$, whereas in other applications the subscript specifies the frequency.] The Fréchet derivative $F(z) = -i\omega\mu_0 f^2(z)$ at $z = \zeta_k$ is determined from

$$f(\zeta_1) = f(0) = -c[\sigma],$$

$$f(\zeta_k) = f(\zeta_1) \prod_{n=1}^{k-1} \frac{\gamma_n + 1/c_n}{\gamma_n + 1/c_{n+1}}\, e^{-\gamma_n d_n}, \qquad k \geqq 2. \tag{4.2}$$

The necessary conditions (2.20) require that at a discontinuity $z = \zeta_k$, different from 0 and $z_2$, $D(z)$ changes sign, i.e.,

$$D(\zeta_k) = w(\zeta_k) + \operatorname{Re}\{\lambda F(\zeta_k)\} = 0, \qquad \zeta_k \neq 0, z_2, \tag{4.3}$$

$D'(\zeta_k) \neq 0$. At $z = z_2$, the conductivity is only discontinuous if $D(z_2 - 0) \cdot D(z_2 + 0) < 0$. The condition (4.3) for each *unknown* discontinuity level, together with the data $c[\sigma] = c$, obviously provide the correct number of equations to compute the positions of the unknown discontinuities and $\lambda$. The examples in Fig. 6 show that there will be up to four unknown levels for the one-frequency case. The dimension of the resulting nonlinear system can again be reduced to four by eliminating $\lambda$ on replacing the four equations (4.3), which are linear in $\lambda$, by two compatibility conditions. These conditions demand that any two of the four ($3 \times 3$) subdeterminants of the augmented ($4 \times 3$) matrix, i.e., $w(\zeta_k)$ as third column, have to vanish.

All extremal models (except the half-space for $S_{max}$, $\psi = 45°$, $\alpha = 1$) terminate with an insulator after a finite number of layers. This pattern changes, when the a priori bound $\sigma_- > 0$ is imposed, because $w(z)$ vanishes for $z > z_2$, and in this range $D(z) = \operatorname{Re}\{\lambda F(z)\}$ will show a kind of damped oscillations rather than tend to a constant. As a consequence, there will be an infinite number of layers, which below a certain level, however, will have an insignificant influence on the actual bounds.

## 5. Conclusion

The explicit examples in Sects. 3 and 4 have demonstrated the possibility of constructing rigorous bounds for $S(z_2)$. But the examples have also shown that the consideration of only a few frequencies yields pessimistic bounds, which might not be very useful in the geophysical application. The situation will even be worse if bounds for spatial averages of the conductivity are constructed rather than for the conductance. Therefore, the joint interpretation of a larger number of frequencies appears to be mandatory. The handling of

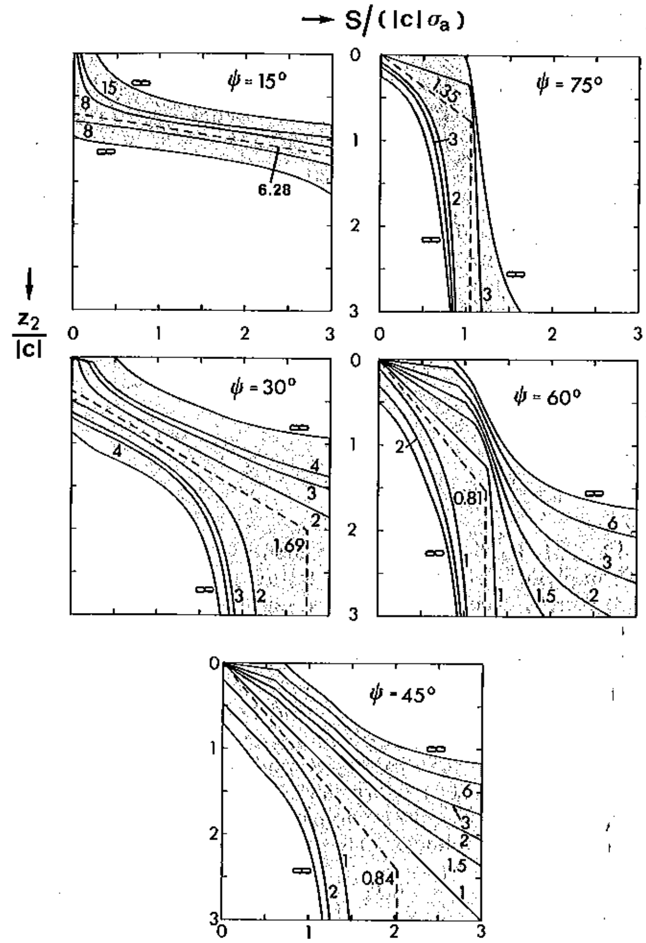


**Fig. 7.** Bounds on $S(z_2)$ in the one-frequency case constrained by $\sigma(z) \leqq \alpha\sigma_a$, where $\alpha$ is the curve parameter. The limiting case $\alpha = \infty$ is already shown in Fig. 2. For the smallest possible value of $\alpha$ there is only one model depicted by the *dashed curve*

many consistent data will not pose serious problems, but an extension of the theory is still necessary to deal with the most interesting case of many real data that are generally inconsistent.

*Acknowledgements.* The author is greatly indebted to one of the referees for pointing out a substantial error in an earlier version of Appendix A. Moreover, the author wishes to thank Prof. H.-J. Dürbaum for providing the opportunity to carry out a major part of the present study at the Federal Institute for Geosciences and Natural Resources (BGR) at Hannover. Many thanks also to Dr. A.G. Jones for making available the results of the COPROD study prior to publication.

## Appendix A: Linear independence of the Fréchet kernels

The simple structure of the extremal models is a result of the assertion that there is no set of $M$ complex constants $\lambda_j$, not all equal zero, so that (2.17) is satisfied in any interval where $w(z)$ is constant and $\sigma(z)$ is positive. The functions $F_j(z) \sim f_j^2(z)$ have to present a downward diffusing field with $F_j'(z) \to 0$ for $z \to z_{\max}$, where $z_{\max}$ is either infinity or the depth to a perfect conductor. This qualification will eliminate the nontrivial solutions of (2.17), which may exist for a particular choice of $\sigma(z)$.

At the beginning it is assumed that at least one interval exists where (2.17) is satisfied and that $a < z < b$ is the deepest. Then (2.17) reads

$$D(z) = w(z) + \operatorname{Re} \sum_{j=1}^{M} \phi_j(z) = 0, \qquad z \in (a, b) \tag{A-1}$$

with $\phi_j(z) := \lambda_j F_j(z)$. For $a < z < b$, the conductivity $\sigma(z)$ is positive. Let $\sigma^{(p)}(b)$, $p \geqq 0$ be the first nonvanishing derivative of $\sigma(z)$ at $z = b - 0$. In $z > b$, a set of $K$ thin sheets of finite conductance may exist, possibly terminated by an additional perfect conductor. For ease of presentation the case $K = 0$ and $K > 0$ are considered separately.

$K = 0$

Let the possible perfect conductor be at $z = b + H$. Differentiate (A-1) $2M$ $(p+2)$ times and evaluate the derivatives at $z = b - 0$ on using $\phi_j'(b) = -(2/H)\ \phi_j(b)$ and the differential equations (2.15a, b). The result is a set of $2M$ homogeneous linear equations for $\operatorname{Re}\phi_j(b)$ and $\operatorname{Im}\phi_j(b)$

$$\operatorname{Re} \sum_{j=1}^{M} (i\omega_j)^n \phi_j(b) = 0, \qquad n = 1, \ldots, 2M, \tag{A-2}$$

where the $n$-th equation is obtained from the $n(p+2)$-th order derivative, observing that this derivative of $\phi_j(z)$ at $z = b - 0$ is of the type

$$\phi_j(b) \sum_{m=0}^{n} \gamma_m (i\omega_j)^m$$

with real frequency-independent coefficients $\gamma_m$ and $\gamma_n \neq 0$. The set (A-2) disintegrates into two uncoupled systems for $\omega_j \operatorname{Im}\phi_j$ and $\omega_j^2 \operatorname{Re}\phi_j$, both having as system determinant the nonvanishing Vandermonde determinant (e.g., Smirnov 1964, p. 21)

$$\Delta = \begin{vmatrix} 1 & \ldots & 1 \\ \omega_1^2 & \ldots & \omega_M^2 \\ \vdots & & \vdots \\ \omega_1^{2M-2} & \ldots & \omega_M^{2M-2} \end{vmatrix} = \prod_{1 \leqq r < s \leqq M} (\omega_s^2 - \omega_r^2) \neq 0. \tag{A-3}$$

Hence, (A-2) allows only the trivial solution $\phi_j(b) = 0$, $j = 1, \ldots, M$. This solution is compatible only with $w(b-0) = 0$ and either a perfect conductor at $z = b$ or $b = \infty$, because the modulus of $\phi_j$ cannot increase with depth. In the first case also $\phi_j'(b) = 0$, but $\phi_j''(b) \neq 0$. Repeating the above arguments for $\phi_j''(b)$ by considering the derivatives of order $n(p+4)$, $n = 1, \ldots, 2M$, it follows that also $\phi_j''(b) = 0$, implying $\phi_j(z) \equiv 0$ in $a < z < b$. In the case $b = \infty$ differentiate (A-1) three times, use (2.15b), divide by $4\mu_0\sqrt{\sigma}$, and integrate to obtain

$$\operatorname{Re} \sum_{j=1}^{M} i\omega_j \sqrt{\sigma(z)}\, \phi_j(z) = \gamma, \qquad z > a, \tag{A-4}$$

where $\gamma$ is a constant. By comparing with power laws $\sigma(z) = Az^m$ leading to Bessel function solutions (or appealing to a bounded energy dissipation), it is always found that

$$\lim_{z \to \infty} \sqrt{\sigma(z)}\, \phi_j(z) = 0,$$

which implies that $\gamma = 0$. Dividing (A-4) by $\sqrt{\sigma}$ and applying the same operations another $(2M-1)$ times, we end up again with the system (A-2), $\phi_j(b)$ being replaced by $\phi_j(z)$. Hence, $\phi_j(z) \equiv 0$ in $z \geqq a$. This shows that for $K = 0$, no solution $\phi_j(z) \not\equiv 0$ of (A-1) can be found.

$K > 0$

Below $z = b$ let there exist $K$ thin sheets of finite conductance $\tau_k$ at $z = \zeta_k$, $k = 1, \ldots, K$ and define $d_1 := \zeta_1 - b \geqq 0$, $d_k := \zeta_k - \zeta_{k-1} > 0$, $k = 2, \ldots, K$. In addition, there may be a perfect conductor at $z=\zeta_K+H$. Separately considered are the cases $w(z)\equiv 0$ in $z\geqq b$ and $w(z)\not\equiv 0$ in $z\geqq b$.

*α) $w(z)\equiv 0$ in $z\geqq b$*

In this case the necessary conditions (3.15a, b) have to be satisfied at all $K$ sheets and lead to the $2K$ equations

$$\operatorname{Re}\sum_{j=1}^{M} e_{2K-n}(\omega_j)\phi_j(\zeta_K)=0, \quad n=0,\ldots,2K-1. \tag{A-5}$$

Working from $z=\zeta_K$ upwards and starting with $e_{2K}=1$, the functions $e_{2K-n}(\omega)$ are, on account of Sect. 3.1 [in particular Eqs. (3.2), (3.4), and (3.5)], recursively defined as

$$\begin{aligned} e_{2k-1}&=e_{2k}(i\omega\mu_0\tau_k-2/c_k),\\ e_{2k-2}&=e_{2k}(1+d_k/c_k)^2 \end{aligned} \tag{A-6}$$

with $k=K,\ldots,1$ and the $c_k$ are obtained by the recurrence relation (3.3), starting with $c_K=H/(1+i\omega\mu_0\tau_K H)$. Examining the structure of $e_{2K-n}(\omega)$, it is easily found that

$$e_{2K-n}(\omega_j)=\sum_{m=0}^{n}\bar{\gamma}_m(i\omega_j)^m, \quad n=0,\ldots,2K-1 \tag{A-7}$$

where $\bar{\gamma}_m$ is again real and frequency independent with $\bar{\gamma}_n\neq 0$. Hence by linear combination (A-5) is equivalent to

$$\operatorname{Re}\sum_{j=1}^{M}(i\omega_j)^n\phi_j(\zeta_K)=0, \quad n=0,\ldots,2K-1. \tag{A-8}$$

For $K\geqq M$ (A-8) implies already $\phi_j(\zeta_K)=0$; for $K<M$ the missing linearly independent equations are obtained from the higher derivatives of $D(z)$ at $z=b-0$. First, let $d_1=\zeta_1'-b>0$. Then the three quantities

$$\begin{aligned} &\phi_j(b)/\phi_j(\zeta_K), \quad \phi_j'(b)/\phi_j(\zeta_K), \quad \text{and}\\ &\phi_j'^2(b)/\{\phi_j(b)\phi_j(\zeta_K)\} \end{aligned} \tag{A-9}$$

are polynomials in $i\omega_j$ of exact degree $2K$. After evaluating the derivatives of $\phi_j(z)$ of order $n(p+2)$, $n=1,\ldots,2M-2K-1$ at $z=b-0$ on, using the preceding result in connection with (A-8) and (2.15a, b), the validity of (A-8) is extended up to powers $2M-1$. As a consequence, $\phi_j(\zeta_K)=0$, implying in fact $\phi_j(z)\equiv 0$. For $d_1=0$ the first two terms of (A-9) are only of degree $2K-2$ and $2K-1$, but the same result is obtained by considering the derivatives of order $-p+n(p+2)$, $n=1,\ldots,2M-2K$.

*β) $w(z)\not\equiv 0$ in $z\geqq b$*

According to Sect. 3.3 the discontinuity of $w(z)$ coincides with the position of a sheet. If this is the sheet $k=1$, then (cf. Sect. 3.3)

$$\begin{aligned} &D(\zeta_1-0)=1, \quad D'(\zeta_1)=0 \quad \text{for } S_{\min},\\ &D(\zeta_1-0)=0, \quad D'(\zeta_1)<0 \quad \text{for } S_{\max} \end{aligned} \tag{A-10}$$

However, $D(b)=0$, $D'(b)=0$ implies $D(z)=A(z-b)^2$ in $b\leqq z\leqq\zeta_1$, which for $d_1\geqq 0$ is incompatible with both cases of (A-10). If the discontinuity occurs at level $k>1$, then

$$D(\zeta_1)=0, \quad D'(\zeta_1-0)<0$$

which again cannot be met by any choice of $A$ for $d_1\geqq 0$.

Summarizing the above results, in the unconstrained case no downward diffusing field solution satisfying (2.17) can be found for $\sigma(z)>0$ in $a<z<b$. The assumption $\sigma(z)>0$ is essential, since for $\sigma(z)\geqq 0$ non-trivial diffusing solutions of (2.17) exist, e.g., $D(z)\equiv 0$ for $z>z_2$ in the case of $S_{\min}$ (cf. Sect. 3.3) without $\phi_j(z)$ vanishing identically.

## Appendix B: Equivalent partial fraction expansions

Let for $M$ distinct frequencies $\omega_j$ the theoretical transfer function $c_j[\sigma]$ of a layered ground be represented by

$$c_j[\sigma]=a_0+\sum_{n=1}^{N}\frac{a_n}{b_n+i\omega_j}, \quad j=1,\ldots,M, \tag{B-1 = 3.10}$$

where the $b_n$ are distinct (otherwise $N$ can be reduced). Assume the ordering $b_n>b_{n+1}$. Then $a_0$ and $b_N$ have to be non-negative, all other constants are strictly positive. The following statement will be proved:

a) For $N\geqq M$ exist two (condensed) representations

$$c_j[\sigma]=\sum_{m=1}^{M}\frac{A_m}{B_m+i\omega_j}, \tag{B-2 = 3.11a}$$

$$c_j[\sigma]=\bar{A}_0+\sum_{n=1}^{M-1}\frac{\bar{A}_m}{\bar{B}_m+i\omega_j}+\frac{\bar{A}_M}{i\omega_j}, \tag{B-3 = 3.11b}$$

$j=1,\ldots,M$. Excluding only the identity $M=N$ with $a_0=b_N=0$, implying also $\bar{A}_0=B_N=0$, the representations (B-2) and (B-3) consist each of $2M$ *positive* constants corresponding to the $2M$ data. There is no representation with less than $2M$ constants, i.e., $B_m$ and $\bar{B}_m$ are distinct.

b) For $N<M$ the representation (B-1) is unique, i.e., no alternative partial fraction expansion exists.

The proof is concentrated on the representation (B-2), and at the end only the necessary modifications for (B-3) are stated. At the outset it is assumed that there is an expansion of type (B-2) with $K\leqq M$ complex terms. Then it has to be shown that the nonlinear system of $2M$ equations

$$\left.\begin{aligned} &\sum_{m=1}^{K}\frac{A_mB_m}{B_m^2+\omega_j^2}=a_0+\sum_{n=1}^{N}\frac{a_nb_n}{b_n^2+\omega_j^2} \quad &\text{(B-4a)}\\ &\sum_{m=1}^{K}\frac{A_m}{B_m^2+\omega_j^2}=\sum_{n=1}^{N}\frac{a_n}{b_n^2+\omega_j^2} \quad &\text{(B-4b)} \end{aligned}\right\} j=1,\ldots,M$$

has $2K$ positive solutions $A_m$, $B_m$, $m=1,\ldots,K$. First, we recall the elementary partial fraction decomposition

$$x^{2k}\Big/\prod_{j=1}^{M}(x^2+\omega_j^2)=\sum_{j=1}^{M}\frac{\alpha_{jk}}{x^2+\omega_j^2}, \quad k=0,\ldots,M-1 \tag{B-5}$$

with

$$\alpha_{jk}=(-\omega_j^2)^k\Big/\prod_{\substack{l=1\\l\neq j}}^{M}(\omega_l^2-\omega_j^2),$$

then multiply (B-4a, b) for $k=0,\ldots,M-1$ by $\alpha_{jk}$, sum over $j$, identify $x$ on the left-hand side with $B_m$, on the right-hand side with $b_n$, and obtain by (B-5) the new set of $2M$ equations

$$\sum_{m=1}^{K}G_mB_m^l=a_0\delta_{l,2M-1}+\sum_{n=1}^{N}g_nb_n^l, \quad l=0,\ldots,2M-1, \tag{B-6}$$

where $\delta_{ik}$ is the Kronecker symbol and

$$G_m:=A_m\Big/\prod_{j=1}^{M}(B_m^2+\omega_j^2), \quad g_n:=a_n\Big/\prod_{j=1}^{M}(b_n^2+\omega_j^2). \tag{B-7}$$

The equations for odd and even $l$ result from (B-4a) and (B-4b), respectively. The quantities $G_m$ rather than $A_m$ may now be considered as unknowns. In the derivation of the first term on the right-hand side it has been observed that by virtue of (B-5)

$$\sum_{j=1}^{M}\alpha_{jk}=\lim_{x\to\infty}x^{2k+2}\Big/\prod_{j=1}^{M}(x^2+\omega_j^2)=\delta_{k,M-1}, \quad k\leqq M-1.$$

The $2M$ equations (B-6) are linear in the $K$ unknowns $G_m$. In order for there to be a solution, any $K+1$ equations of (B-6) have to be linearly dependent. Taking, for instance, the $K+1$ equations from $l=i$ to $l=i+K$, $i=0, \ldots, 2M-K-1$, then for each $i$ there has to be a set of coefficients $q_k^{(i)}$, $k=0, \ldots, K$, not all equal to zero, such that

$$\sum_{k=0}^{K} q_k^{(i)} B_m^{i+k}=0, \quad m=1, \ldots, K, \tag{B-8a}$$

$$a_0 q_K^{(i)} \delta_{i,2M-K-1}+\sum_{k=0}^{K} q_k^{(i)} \sum_{n=1}^{N} g_n b_n^{i+k}=0. \tag{B-8b}$$

Since we are searching for positive $B_m$, (B-8a) may be divided by $B_m^i$ to yield

$$\sum_{n=0}^{K} q_k^{(i)} B_m^k=0, \quad m=1, \ldots, K. \tag{B-8c}$$

$q_k^{(i)}$ is independent of $m$. Hence, each $B_m$ satisfies the same algebraic $K$-th order equation, i.e., by the fundamental theorem of algebra the existence of the set $q_k^{(i)}$ implies the existence of solutions $B_m$ being the $K$ roots $z$ of

$$\sum_{k=0}^{K} q_k^{(i)} z^k=0. \tag{B-9}$$

On the other hand, the roots define the coefficients $q_k^{(i)}$ uniquely apart from a scaling factor. Therefore, the $q_k^{(i)}$ are in fact independent of $i$, $q_k^{(i)}=q_k$. Normalizing by $q_K=1$, the remaining $K$ coefficients $q_k$ have to be determined from the $2M-K$ linear equations (B-8b). First, let $K=M$. Then the system determinant

$$\Delta_M=\det\left\{\sum_{n=1}^{N} g_n b_n^{k+i}\right\}, \quad i,k=0, \ldots, M-1 \tag{B-10}$$

can be expressed for $N \geqq M$ as

$$\Delta_M=\sum\left\{\prod_{k=1}^{M} g_{n_k}\right\} \cdot \begin{vmatrix} 1 & b_{n_1} & \ldots & b_{n_1}^{M-1} \\ \vdots & \vdots & & \vdots \\ 1 & b_{n_M} & \ldots & b_{n_M}^{M-1} \end{vmatrix}^2, \tag{B-11}$$

where the summation extends over all $M$-tupels $n_k$, $k=1, \ldots, M$ with $1 \leqq n_1<\ldots<n_M \leqq N$ (e.g., Smirnov, 1964, p. 28). The determinants in (B-11) are again Vandermonde determinants, which are generally defined as $V=\det\{x_j^{k-1}\}$, $j,k=1, \ldots, M$ and are given by (e.g., Smirnov, 1964, p. 21)

$$V=\prod_{1 \leqq p<q \leqq M}(x_q-x_p). \tag{B-12}$$

All terms in the sum (B-11) are positive by virtue of the assumptions $N \geqq M$ and $b_n$ distinct. Hence, $\Delta_M>0$ and the coefficients $q_k$ can be determined uniquely. In the case $N<M$, however, $\Delta_M=0$, as is seen by formally adding in (B-10) $M-N$ terms with $g_{N+1}=\ldots=g_M=0$ and using (B-11). In this case there is no set of coefficients $q_k$, implying that (B-1) cannot be modified.

The case of $K<M \leqq N$ must still be discussed, in which the linear system (B-8b) consists of $2M-K=K+2(M-K)$ equations for only $K$ unknowns. A necessary condition for the existence of a solution is the linear dependence of the first $K+1$ equations, which is equivalent to the statement that $\Delta_{K+1}=0$. However, (B-11) with $M=K+1$ shows that $\Delta_{K+1}>0$. Hence, for $K<M$ the first $K+1$ equations are already linearly independent and there is no solution $q_k$. Therefore, in the sequel only the case $K=M$, $N \geqq M$ has to be considered.

Having established the existence of the set $B_m$ as the roots of (B-9) with $K=M$, we have to show that $B_m$ is real and positive. Without exploiting (B-9) any further, we return to (B-8b, c). In order for there to be a solution $q_k^{(i)} \equiv q_k$, $k=0, \ldots, M$ for this homogeneous linear system, the determinant has to vanish, implying

$$a_0 \delta_{i,M-1} \begin{vmatrix} 1 & B_1 & \ldots & B_1^{M-1} \\ \vdots & \vdots & & \vdots \\ 1 & B_M & \ldots & B_M^{M-1} \end{vmatrix}+\sum_{n=1}^{N} g_n b_n^i \begin{vmatrix} 1 & B_1 & \ldots & B_1^M \\ \vdots & \vdots & & \vdots \\ 1 & B_M & \ldots & B_M^M \\ 1 & b_n & \ldots & b_n^M \end{vmatrix}=0,$$

$i=0, \ldots, M-1$. The above Vandermonde determinants are easily evaluated by (B-12) and yield after much cancellation since the $B_m$ are distinct

$$a_0 \delta_{i,M-1}+\sum_{n=1}^{N} g_n b_n^i \prod_{m=1}^{M}(b_n-B_m)=0, \quad i=0, \ldots, M-1, \tag{B-13}$$

or equivalently

$$a_0 \gamma_{M-1}+\sum_{n=1}^{N} g_n p_{M-1}(b_n) \prod_{m=1}^{M}(b_n-B_m)=0, \tag{B-14}$$

where $p_{M-1}(b_n)$ is an *arbitrary* polynomial in $b_n$ of degree *not higher* than $M-1$ with $\gamma_{M-1}$ as coefficient of $b_n^{M-1}$. The $M$ equations (B-13) form a nonlinear system for $B_m$. The existence of a solution set $B_m$ is granted from (B-8c) and (B-9). To show the positivity of the particular element $B_k$, $k=1, \ldots, M$, we take

$$p_{M-1}(b_n)=\prod_{m=1}^{M}{}'(b_n-B_m^*), \quad \gamma_{M-1}=1,$$

where prime and asterisk denote, respectively, the omission of the factor $m=k$ and the complex conjugate, and obtain from (B-14)

$$a_0+\sum_{n=1}^{N} g_n(b_n-B_k) \prod_{m=1}^{M}{}' |b_n-B_m|^2=0. \tag{B-15}$$

This shows that $B_k$ is real and positive.

Next it is proved that also $A_k$ [or $G_k$, cf. Eq. (B-7)] is positive. The solution of the first $M$ equations of (B-6) for $G_k$ yields by Cramer's rule on exploiting, again the simple properties of the resulting Vandermonde determinants

$$G_k=\sum_{n=1}^{N} g_n \prod_{m=1}^{M}{}' \frac{b_n-B_m}{B_k-B_m}. \tag{B-16}$$

The definite sign of $G_k$ is not yet obvious. However, expanding the product by

$$\prod_{m=1}^{M}{}'(B_k-B_m)=\prod_{m=1}^{M}{}'[(b_n-B_m)-(b_n-B_k)]$$
$$=(b_n-B_k) p_{M-1}(b_n)+\prod_{m=1}^{M}{}'(b_n-B_m), \tag{B-17}$$

where $p_{M-1}$ is, in fact, a polynomial of degree $M-2$, we obtain from (B-16) by means of (B-14) with $\gamma_{M-1}=0$:

$$G_k=\sum_{n=1}^{N} g_n \prod_{m=1}^{M}{}'\left(\frac{b_n-B_m}{B_k-B_m}\right)^2>0. \tag{B-18}$$

This proves the existence of the representation (B-2).

Skipping details of derivation, we mention only two additional identities required in Sect. 3.2:

$$\sum_{m=1}^{M}(A_m-2a_0 B_m)=\sum_{n=1}^{N}\left[a_n-g_n \prod_{m=1}^{M}(b_n-B_m)^2\right], \tag{B-19}$$

$$\sum_{m=1}^{M}(A_m/B_m)=a_0+\sum_{n=1}^{N}(a_n/b_n)$$
$$-\prod_{j=1}^{M}(\omega_j/B_j)^2 \cdot\left[a_0+\sum_{n=1}^{N}(g_n/b_n) \prod_{m=1}^{M}(b_n-B_m)^2\right]. \tag{B-20}$$

The existence of the representation (B-3) is proved similarly. The equivalents of (B-6), (B-13), and (B-14) are

$$\sum_{m=1}^{M-1} \bar{G}_m \bar{B}_m^l + \bar{G}_M \delta_{l0}$$

$$= (a_0 - \bar{A}_0)\delta_{l,2M-1} + \sum_{n=1}^{N} g_n b_n^l, \quad l=0, \ldots, 2M-1, \qquad \text{(B-21)}$$

$$(a_0 - \bar{A}_0)\delta_{iM} + \sum_{n=1}^{N} g_n b_n^i \prod_{m=1}^{M-1} (b_n - \bar{B}_m) = 0,$$

$$i = 1, \ldots, M, \qquad \text{(B-22)}$$

$$(a_0 - \bar{A}_0)\gamma_{M-1} + \sum_{n=1}^{N} g_n p_{M-1}(b_n) b_n \prod_{m=1}^{M-1} (b_n - \bar{B}_m) = 0. \qquad \text{(B-23)}$$

The positivity of $\bar{B}_k$, $k=1, \ldots, M-1$, is proved by taking

$$p_{M-1}(b_n) = \prod_{m=1}^{M-1}{}' (b_n - \bar{B}_m^*), \qquad \gamma_{M-1} = 0,$$

implying

$$\sum_{n=1}^{N} g_n (b_n - \bar{B}_k) \prod_{m=1}^{M-1}{}' |b_n - \bar{B}_m|^2 = 0$$

and $b_1 \geqq \bar{B}_k \geqq b_N$. Choosing

$$p_{M-1}(b_n) = \prod_{m=1}^{M-1} (b_n - \bar{B}_m), \qquad \gamma_{M-1} = 1$$

we obtain

$$\bar{A}_0 = a_0 + \sum_{n=1}^{N} g_n b_n \prod_{m=1}^{M-1} (b_n - \bar{B}_m)^2 > 0. \qquad \text{(B-24)}$$

Finally, $\bar{G}_m$ is found by solving the first $M$ equations of (B-21) for $\bar{G}_m$ and using analogues of the identity (B-17):

$$\bar{G}_k \bar{B}_k = \prod_{n=1}^{N} g_n b_n \prod_{m=1}^{M-1}{}' \left(\frac{b_n - \bar{B}_m}{\bar{B}_k - \bar{B}_m}\right)^2 > 0, \quad k=1, \ldots, M-1, \qquad \text{(B-25)}$$

$$\bar{G}_M = \sum_{n=1}^{N} g_n \prod_{m=1}^{M-1} \left(\frac{b_n - \bar{B}_m}{\bar{B}_m}\right)^2 > 0. \qquad \text{(B-26)}$$

## References


Anderssen, R.S., Seneta, E.: A simple statistical estimation procedure for Monte Carlo inversion in geophysics. Pure Appl. Geophys., **91**, 5–13, 1971

Anderssen, R.S., Seneta, E: A simple statistical estimation procedure for Monte Carlo inversion in geophysics. II: Efficiency and Hempel's paradox. Pure Appl. Geophys., **96**, 5–14, 1972

Barcilon, V.: Ideal solution of an inverse normal mode problem with finite spectral data. Geophys. J. R. Astron. Soc., **56**, 399–408, 1979

Barcilon, V., Turchetti, G.: On an inverse eigenvalue problem with truncated spectral data. In: Inverse and improperly posed problems in differential equations, G. Anger, ed.: pp. 25–34, Berlin: Akademie-Verlag 1979

Brown, K.M.: Computer oriented algorithms for solving systems of simultaneous nonlinear algebraic equations, G.D. Byrne, C.A. Hall, ed.: pp. 281–348. New York and London: Academic Press 1973

Jones, A.G.: Report on the COPROD study. Paper read at the Fifth Workshop on Electromagnetic Induction in the Earth and Moon, Istanbul, August 18–23, 1980

Lawson, C.L., Hanson, R.J.: Solving least squares problems. Englewood Cliffs: Prentice-Hall 1974

Oldenburg, D.W.: Funnel functions in linear and non-linear appraisal. J. Geophys. Res., **88**, 7387–7398, 1983

Parker, R.L.: Inverse theory with grossly inadequate data. Geophys. J. R. Astron. Soc., **29**, 123–138, 1972

Parker, R.L.: Best bounds on density and depth from gravity data, Geophysics, **39**, 644–649, 1974

Parker, R.L.: The theory of ideal bodies for gravity interpretations. Geophys. J. R. Astron. Soc., **42**, 315–334, 1975

Parker, R.L.: The Fréchet derivative for the one-dimensional electromagnetic induction problem. Geophys. J. R. Astron. Soc., **49**, 543–547, 1977

Parker, R.L.: The inverse problem of electromagnetic induction: existence and construction of solutions based on incomplete data. J. Geophys. Res., **85**, 4421–4428, 1980

Parker, R.L.: The existence of a region inaccessible to magnetotelluric sounding. Geophys. J. R. Astron. Soc., **68**, 165–170, 1982

Parker, R.L., Whaler, K.A.: Numerical methods for establishing solutions to the inverse problem of electromagnetic induction. J. Geophys. Res., **86**, 9574–9584, 1981

Pearson, C.E. [ed.]: Handbook of applied mathematics. New York: Van Nostrand Reinhold Co. 1974

Sabatier, P.C.: On extremal solutions of Sturm-Liouville inverse problems. In: Inverse and improperly posed problems in differential equations, G. Anger, ed.: pp. 223–231. Berlin: Akademie-Verlag 1979

Schmucker, U.: Anomalies of geomagnetic variations in the southwestern United States. Bull. Scripps Inst. Oceanogr. **13**, 1–165, 1970

Schmucker, U.: EM-Übertragungsfunktionen für Sq. In: Protokoll Kolloqu. „Erdmagnetische Tiefenforschung" in Grafrath March 19–23, 1984, J. Homilius and V. Haak, ed., Hannover: Niedersächsisches Landesamt für Bodenforschung 1984

Smirnov, V.I.: A course of higher mathematics, Vol. III/1. Oxford [etc.]: Pergamon Press 1964

Weidelt, P.: The inverse problem of geomagnetic induction. Z. f. Geophys., **38**, 257–289, 1972.

Weidelt, P.: Extremal models for electromagnetic induction in two-dimensional perfect conductors. J. Geophys., **49**, 217–225, 1981


Received October 1, 1984; Revised August 1, 1985
Accepted August 1, 1985